LA-UR- 03 - 3537

Approved for public release; distribution is unlimited.

Title: Improving the LLNL Pulsed Sphere Experiments Database and MCNP Models

Author(s): J. A. Bucholz (Oak Ridge National Laboratory)
S. C. Frankle (LANL X-5)

Submitted to: To Be Presented at the 2003 American Nuclear Society Annual Meeting, San Diego, CA, June 1-5

Improving the LLNL Pulsed Sphere Experiments Database and MCNP Models

J. A. Bucholz (ORNL)
and
S. C. Frankle (LANL)

ANS Meeting in San Diego, June 1- 5, 2003

ABSTRACT

From the late 1960s to about 1985, a large number of pulsed-sphere experiments were performed at the Lawrence Livermore National Laboratory (LLNL) in which small, medium, and large spheres of 32 different materials were pulsed with a burst of 14 MeV neutrons. Measured time-dependent detector responses at distant locations provide benchmark spectra by which various neutron transport codes and cross-section libraries may be judged.

The first objective of this study was to: (a) review all of the data from LLNL's "ExptData" and "Disp93in" experimental datafiles, (b) extract only the most reliable and most encompassing results, and (c) create a well-documented Master Library for the high-energy measurements. This includes data on the pulsed-sphere geometries, the materials, various experimental parameters, and the measured neutron spectra vs time and energy. The resulting Master Library included information on 145 high-energy detector measurements, including measurements made on 75 different spheres made of 32 different materials.

The second objective was to improve and refine the existing MCNP models of those experiments as much as possible. (1) The target assembly, previously ignored in all past models, was explicitly included in these newer models. (2) It was verified that more realistic models using beamline collimators gave results that were significantly different from the uncollimated models previously used, especially in the 10-12 MeV range. (3) Reflection off the walls of the vault was evaluated and found to have a negligible effect. (4) The effect of modeling the collimators as concrete or as neutronically black absorbers was also investigated, with mixed results. (5) Marchetti's new space-energy-direction-dependent source terms were found to give much better results in the 12-15 MeV range than the traditional source term specifications.

Using these improved models, the third objective was to compare the calculated MCNP results using the ENDF60, ENDF66, and ENDL92 cross-section libraries against the experimentally measured neutron spectra for 76 (of the 145) detector measurements in the high-energy Master Library. These include measurements made on 36 (of the 75) pulsed-sphere configurations involving 20 (of the 32) different materials. In general: (1) The ENDL92 results appear better than the ENDF results at higher energies above 10 MeV, while the ENDF results appear to be better at lower energies below 10 MeV. (2) The ENDF60 and ENDF66 results generally appear to be indistinguishable for the materials, energies, and flight times studied.

Purpose of Study

- **Survey literature and existing databases (ExptData and Disp93in), and develop a new "Master Library" of high-energy experiments.**

- **To investigate modeling approximations and upgrade existing models.**

- **To compare calculated MCNP results using ENDF60, ENDF66 and ENDL92 xsect data against experimental measurements.**

The Experimental Layout

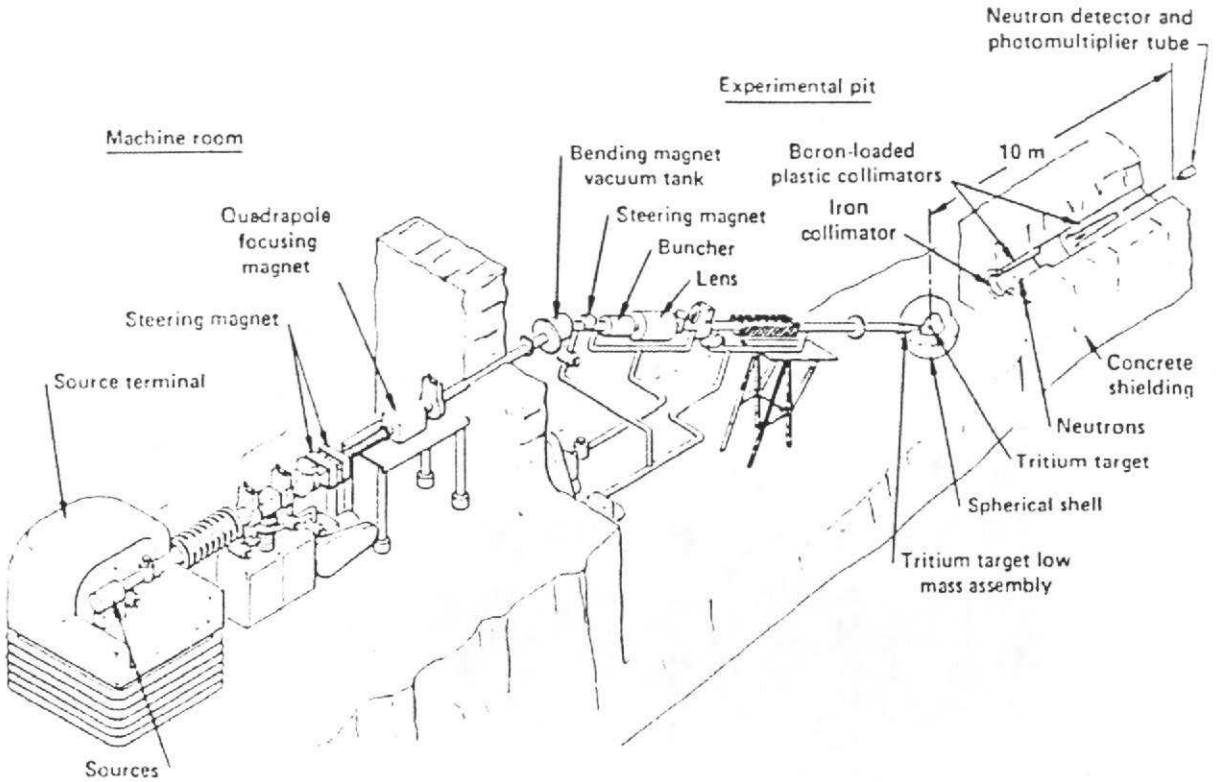

Fig. 1. Schematic view of the accelerator, beam transport, target sphere, collimator, and detector assembly (not to scale). Taken from page 3 of UCLR-ID-131461.

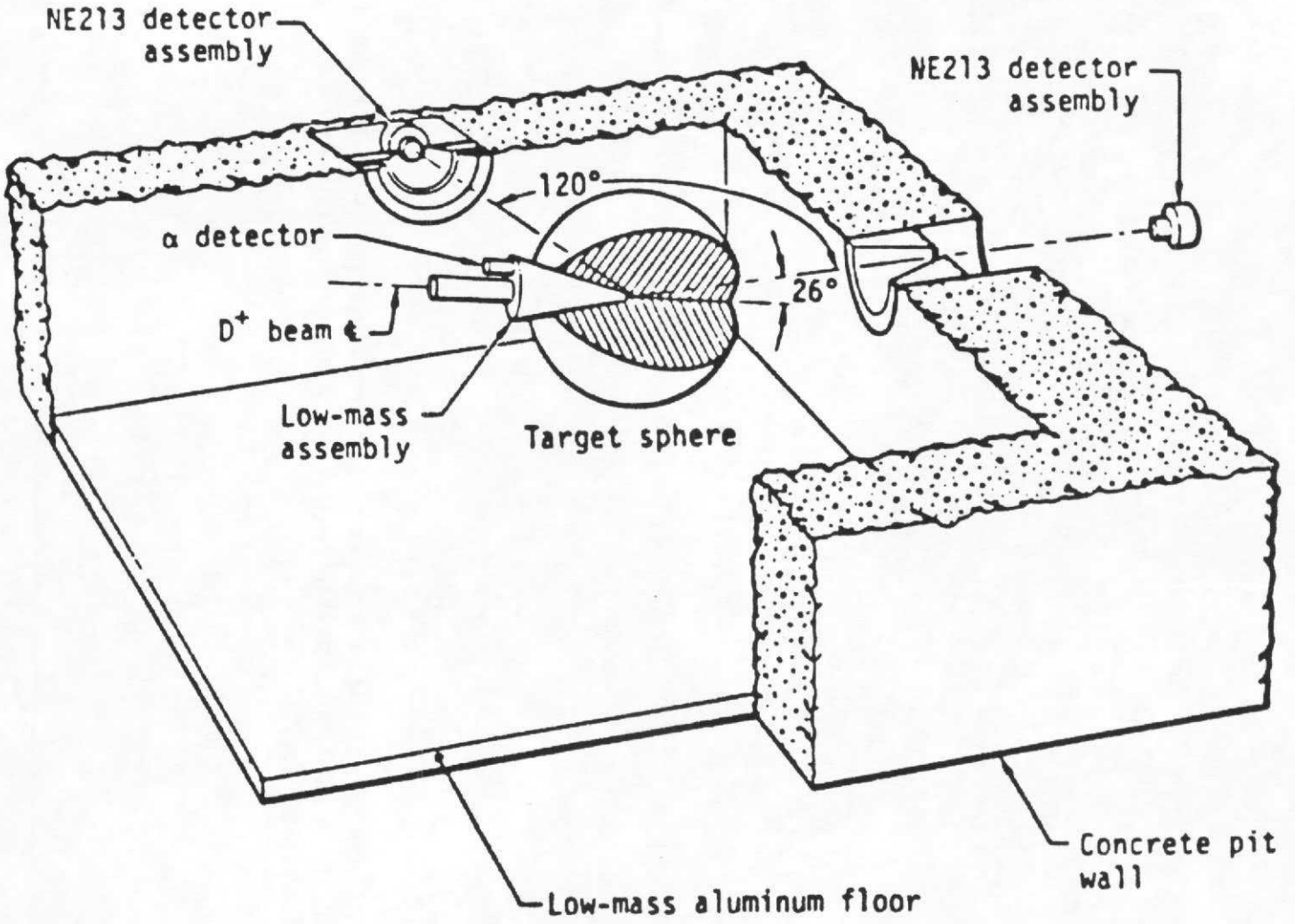

Fig. 2a. Schematic drawing of the pulsed sphere equipment room at the Lawrence Livermore National Lab. Shows time-of-flight geometry for the target spheres and collimated neutron detectors. Taken from page 72 of UCID-17332 and page 7 of LA-12212.

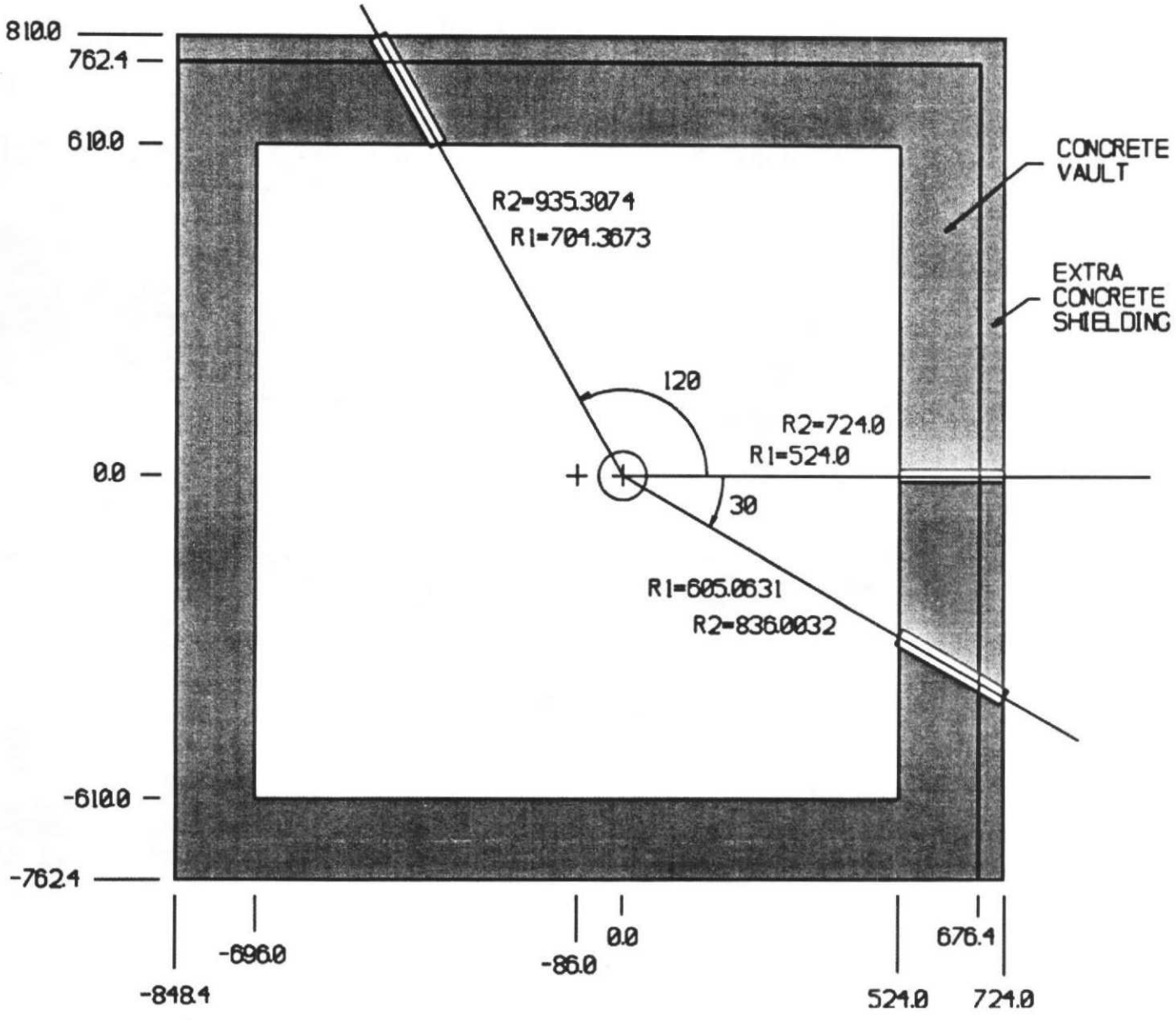

Fig. 2b. Dimensions of the pulsed sphere equipment room (target pit) in cm, and the location of the sphere(s) inside that room. Here R1 and R2 denote the beginning and ending locations of the concrete wall relative to the center of the sphere along each of the three beamlines.

Some Typical Spheres

Types of Spheres

- Many are "very simple", like the 0.9 mfp AL sphere
- Some are clad with SS; a couple are clad with Cd, like the 1.3 mfp Pu-239 sphere
- Some are hollow spheres, like the 0.8 mfp Be sphere
- Some "look weird", like the 3.5 mfp Be sphere
- Some are made of 2 to 6 SS-clad hemispherical shells, like the 1.6 mfp Li-6 sphere
- The liquid-filled spheres are inside a spherical vacuum bottle, like the 1.1 mfp liquid Nitrogen sphere

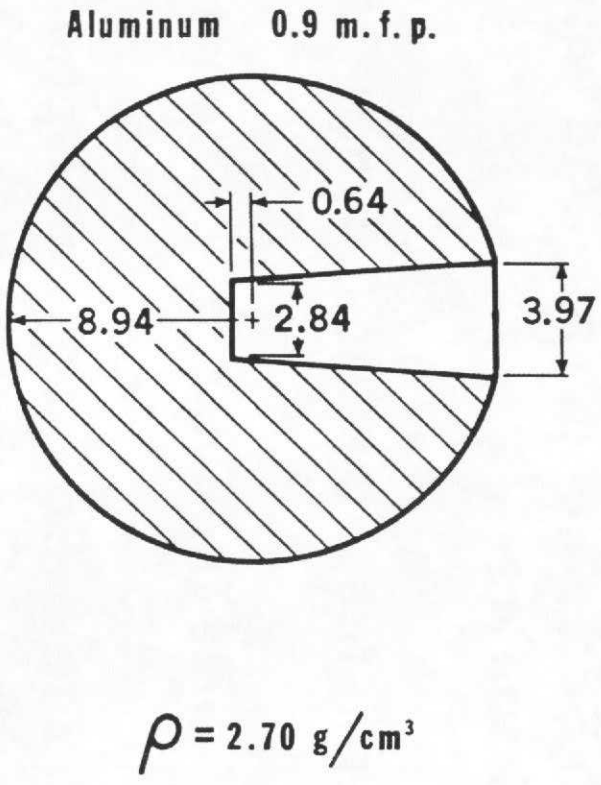

Fig. 10. Aluminum sphere, 0.9 mfp (AL0.9). Used for detector measurements DM033-DM034. All dimensions are in cm. Taken from page 161 of UCLR-51144, Rev I.

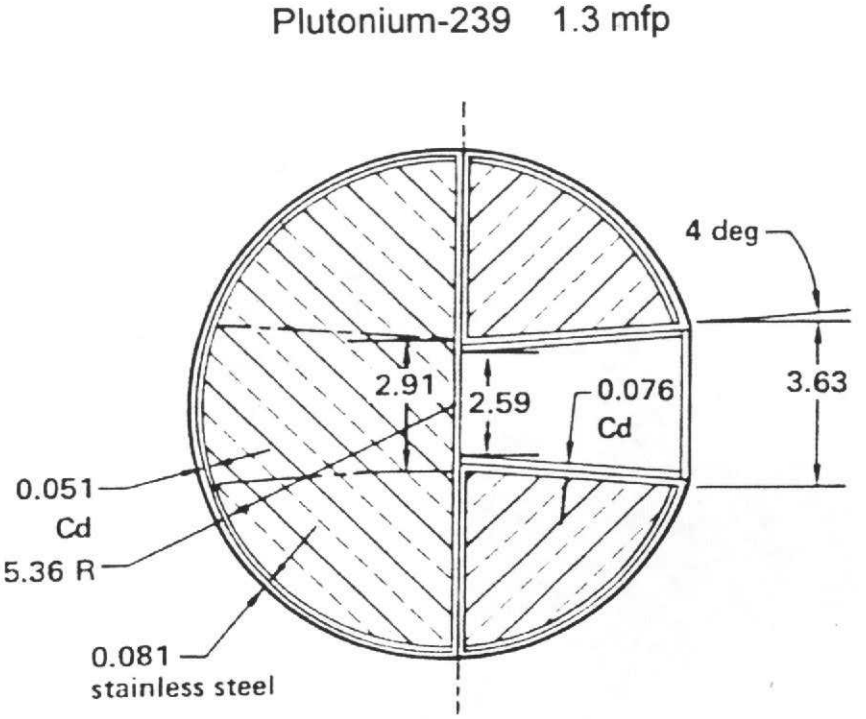

Fig. 46. Plutonium-239 sphere, 1.3 mfp (49P1.3). Used for detector measurements DM120-DM121. All dimensions are in cm. Taken from (and assumed to be the same as) the 1.25 mfp Cd-covered sphere shown in Fig. 1b on page 37 of NS&E, Vol 72 (1979).

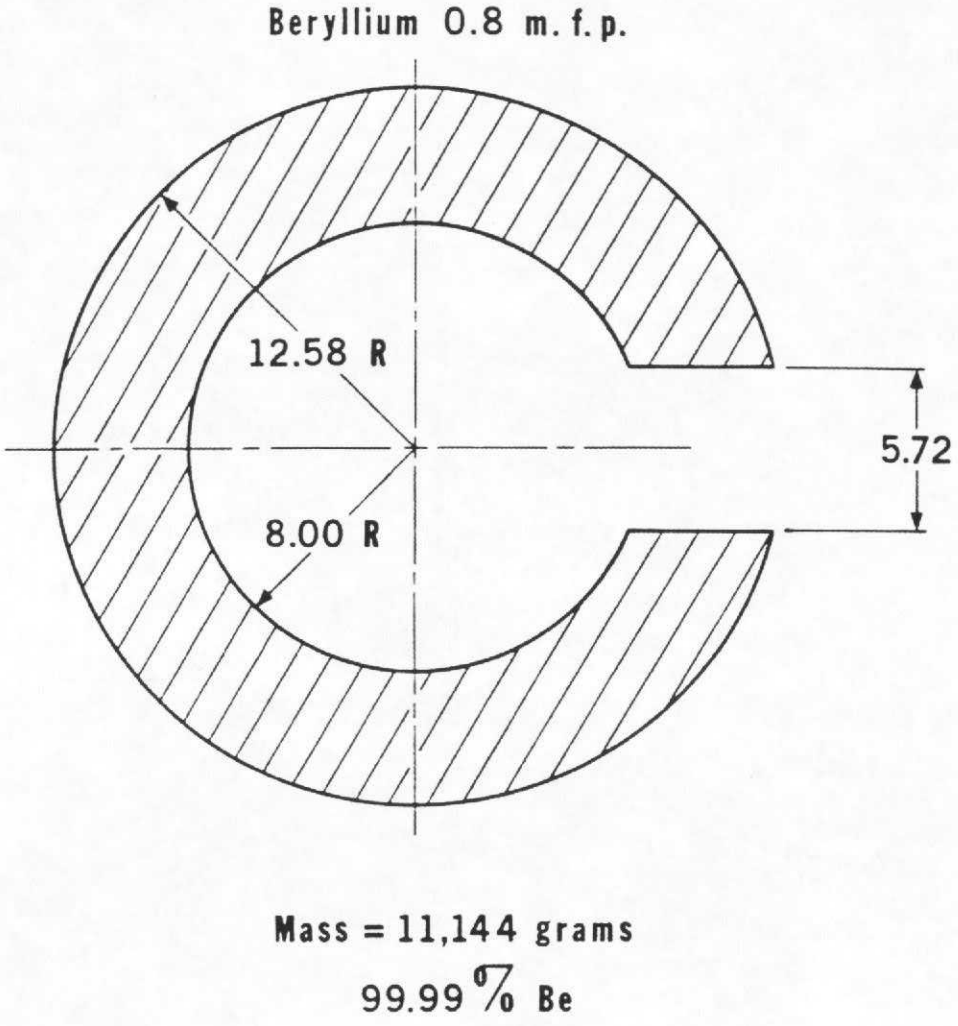

Fig. 14. Beryllium sphere, 0.8 mfp (Be0.8). Used for detector measurements DM039-DM044. All dimensions are in cm. Taken from page 85 of UCLR-51144, Rev I.

Beryllium 3.5 mfp

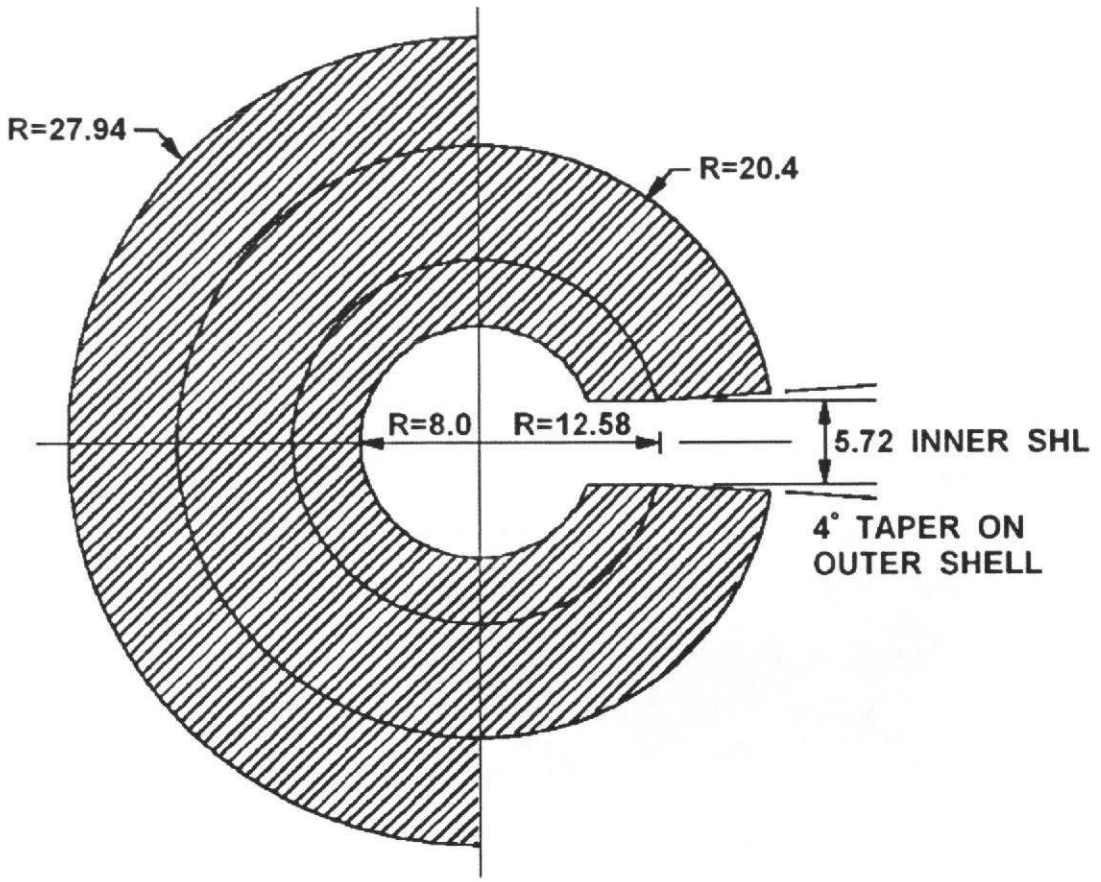

ρ(Be) = 1.83 g/cc (100% Be-9)

R_{max} = 27.9 cm (as per page 1 of UCRL-91774)
R_{max} = 27.94 cm (as per pp 35-38 of UCRL-ID-131461)
Mass not given either place.

Fig. 10. Berylliym sphere, 3.5 mfp (Be 3.5). Used for detector measurements M 50-DM 053. All dimensions are in cm. Modeled as per verbal description on page 1 of UCRL-91 74 (Apr 1985).

Lithium-6 1.6 mfp

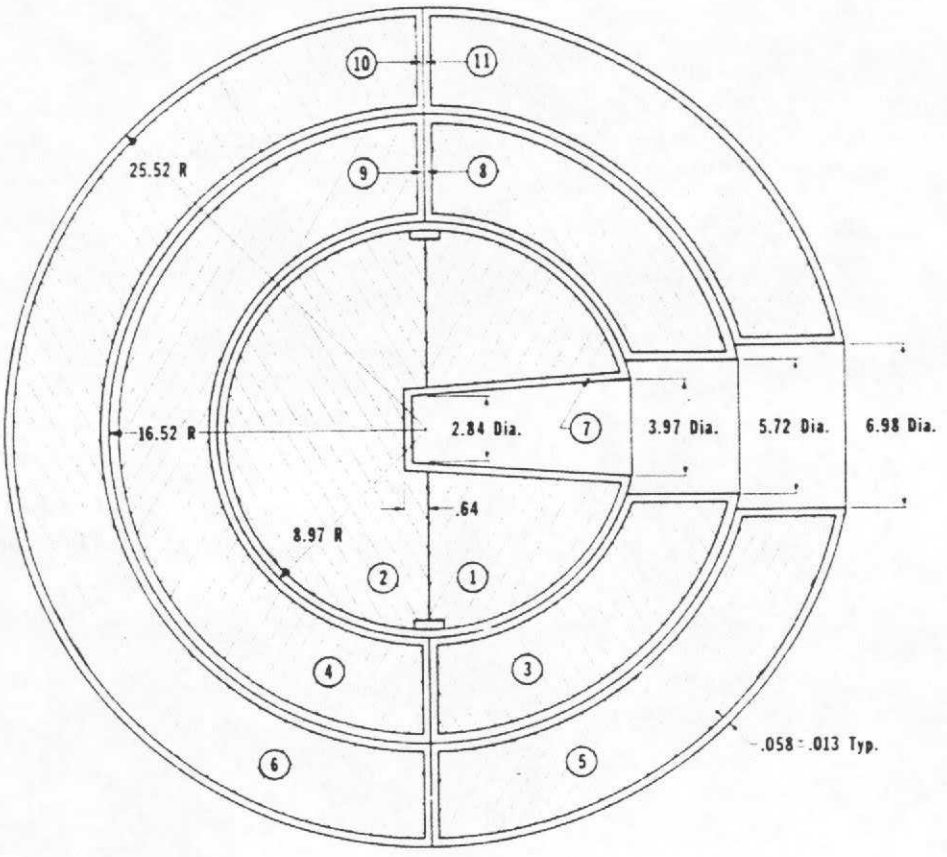

zone	Mass in grams	Material
1	629	
2	668	^{6}Li – 95.0%
3	3337	
4	3450	^{7}Li – 5.0%
5	11060	
6	11207	
7	578	Fe – 68.6%
8	2930	Cr – 20.0%
9	2871	Ni – 8.4%
10	6340	Si – 2.0%
11	6295	Mn – 1.0%

Fig. 3. Lithium-6 sphere, 1.6 mfp (6Li1.6). Used for detector measurements DM007-DM008. All dimensions are in cm. Taken from page 57 of UCLR-51144, Rev I.

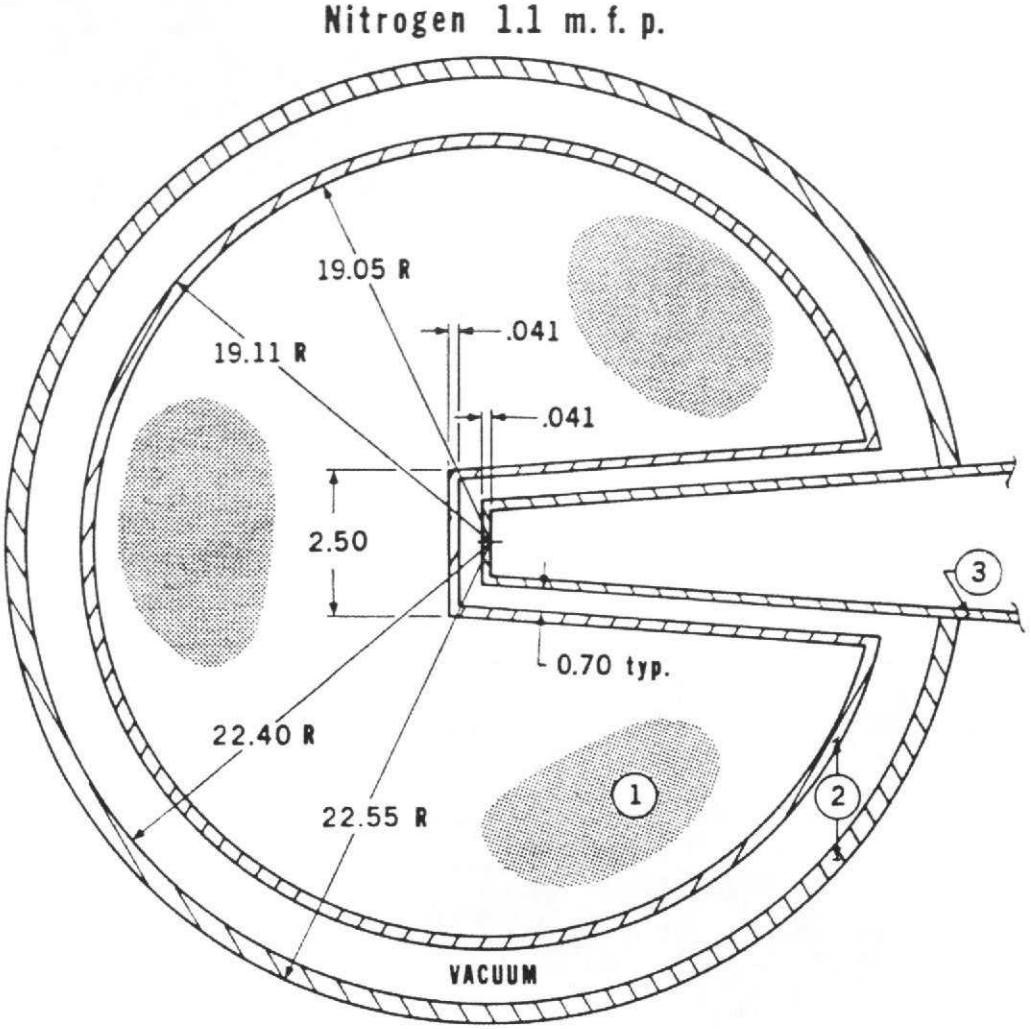

Zone	Density (g/cm^3)	Material	Atomic %
1	0.808	Liquid N_2	100.0
2	7.9	Fe	68.6
		Cr	20.0
		Ni	8.4
		Si	2.0
		Mn	1.0
3	I.C.T. Low Mass Ass'y and Target (See Fig.6, Sect. 1)		

Fig. 37. Liquid nitrogen sphere, 1.1 mfp (N1.1). Used for detector measurements DM101-DM102. All dimensions are in cm. Taken from page 121 of UCLR-51144, Rev I, but also shown on page 74 of UCID-17332, and in Fig. 1d on page 321 of NS&E, Vol 105 (1990). This also corresponds to the 1 mfp sphere shown in Fig. 1 on page 551 of NS&E, Vol 62 (1977).

Target Assemply (placed in each sphere)

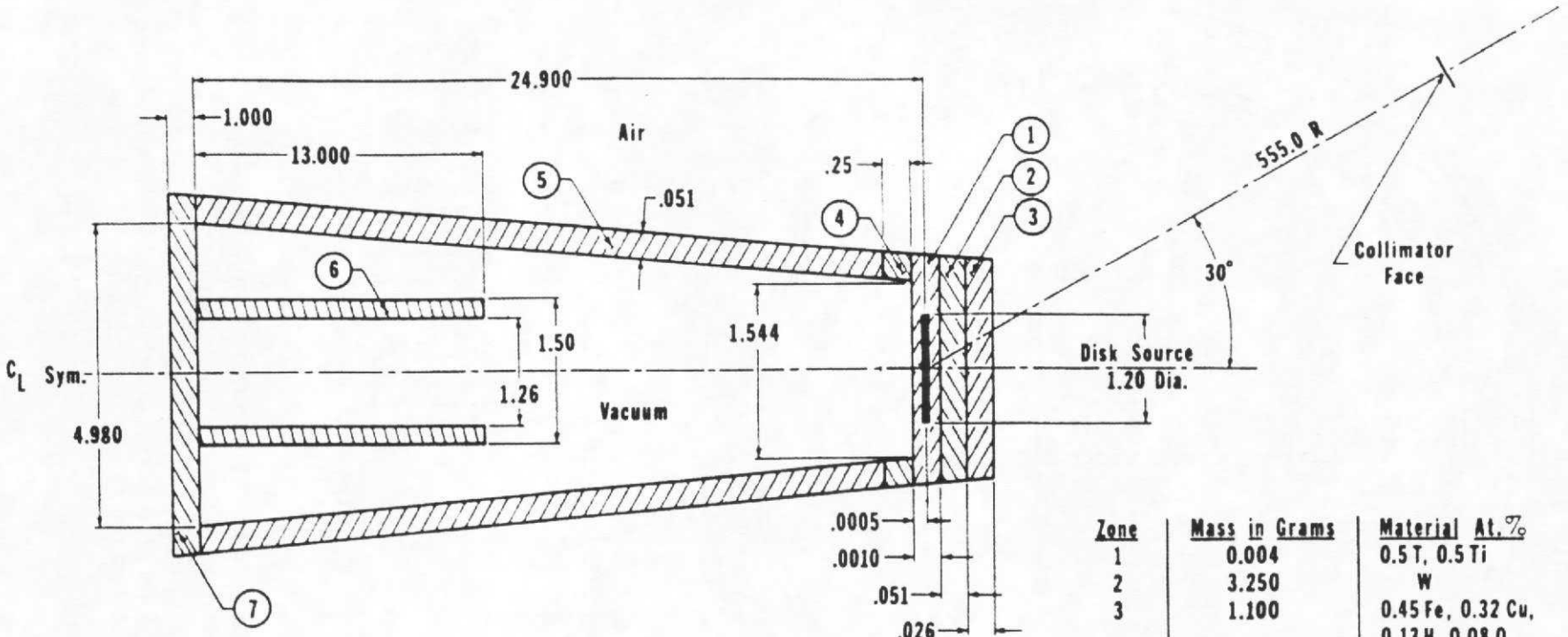

Zone	Mass in Grams	Material At.%
1	0.004	0.5 T, 0.5 Ti
2	3.250	W
3	1.100	0.45 Fe, 0.32 Cu, 0.13 H, 0.08 O, 0.02 Al, 0.06 C
4	1.500	0.5 Al, 0.3 H, 0.2 C
5	35.600	Al
6	18.300	Al
7	417.000	0.5 Al, 0.5 Cu

Ti–T TARGET ASSEMBLY SCHEMATIC

Fig. 3. Idealized model of the titanium-trituim target assembly used in the pulsed sphere experiments. Taken from page 10 of UCLR-5114, Rev I.

TOTAL NUMBER OF CASES

145 detector measurements	(76 calculated)
75 different spheres of	(36 calculated)
32 different materials	(20 calculated)

LIST OF MATERIALS

20 materials calculated already	12 materials not yet calculated
Li-6	LiD
Li-7	Gold
AL	Cu
Be-9	Ho
C	L.Air
Poly	Nb
Conc	Tin
Fe	Ta
Mg	Th232
L.Nit	
L.Oxy	
Pb	* LiH
Pu239	* FibGL
Tef	* Mo
Ti	
W	* geometry
U-235	unknown for
U-238	7 configs
HWtr	using these
LWtr	3 matls

The Master Library

of high-energy experiments

The Master Library of high-energy experiments

Primary Literature References:

- UCRL-51144, Rev. I (Feb 1972), on LLNL pulsed sph pgm
- UCRL-ID-131461 (July 1998), by A. Marchetti
- Numerous other reports & journal articles

Primary Data References:

- EXPTDATA file (from LLNL to LANL; early 1990s)
- DISP93IN file (from LLNL to LANL; late 1990s)

Objectives of the new high-energy Master Library

- Combine data from past compilations (ExptData & Disp93in); ExptData has 109 experiments; Disp93in has 71; both are incomplete and partially overlappping

- Eliminate any flawed data; resolve discrepancies

- Eliminate redundant datasets; for repeated experiments, keep datasets with wider range of times or energies

- Keep only data related to high-energy measurements; data for low-energy measurements will be treated later

Elements of the new high-energy Master Library

- Summary-level INDEX of 145 detector measurements on 75 pulsed spheres made of 32 different materials; gives all key parameters unique to each measurement

- DMxxx Data Files give key parameters & all of the time-dependent / energy-dependent / measured data

- DMxxx.doc Text Files give
  - -- additional comments on expt data (why set was chosen)
  - -- extensive comments on MCNP models (when they exist)

- Figures for 68 of the pulsed spheres (7 configs still missing)
  - -- biggest collection ever in any one place
  - -- geometry, dimensions, materials, masses, den. etc
  - -- frequently give 1 or 2 or 3 additional references

INDEX of 145 High-Energy Detector Measurements

Table 1. Summary of key information about each pulsed sphere detector measurement (DMxxx) in the Master Library. The corresponding DMxxx file in the Master Library contains the experimentally measured count rates as a function of flight-time and energy, while the corresponding DMxxx.TXT file contains additional comments about both the experimental data and the MCNP model. Highly descriptive figures (6Li0.5.jpg, etc) are included in this report, or on the accompanying CD, for all but the LiH, Mo, and fiberglass spheres.

Det Meas. ID #	MCNP Input File	Input File Done?	Sph Matl	Size (mfp)	Outer Radius (cm)	FWHM (ns)	Beam Line ID	Beam Ang wrt the Src(deg)	Flight Path (cm)	Detector Type	Det Bias MeV	Npts	Tmin (ns)	Tmax (ns)	ExptData ID #	Disp93in ID #	Reference Publication
DM001	6Li0.5a	Yes	Li-6	0.5	8.970	4	30	38.8877	765.2	Pilot B	1.6	138	135.00	409.00	1	------	UCRL-51144
DM002	6Li0.5b	Yes	Li-6	0.5	8.970	4	120	116.7050	977.2	NE213-A	1.6	162	185.00	507.00	2	------	UCRL-51144
DM003	6Li0.5c	Yes	Li-6	0.5	8.970	2	26	26.0	746.34	NE213-B	1.6	170	129.00	467.00	102506	300602176	UCRL-ID-131461
DM004	6Li1.1a	No	Li-6	1.1	16.520	2	26	26.0	746.34	NE213-B	1.6	178	129.00	483.00	102605	------	-------
DM005	6Li1.1b	No	Li-6	1.1	16.520	4	30	38.8877	765.2	Pilot B	1.6	138	135.00	409.00	3	------	UCRL-51144
DM006	6Li1.1c	No	Li-6	1.1	16.520	2	26	26.0	878.0	Stilbene	0.8	364	149.00	875.00	------	300604180	-------
DM007	6Li1.6a	Yes	Li-6	1.6	25.520	4	30	38.8877	765.2	Pilot B	1.6	139	133.00	409.00	4	------	UCRL-51144
DM008	6Li1.6b	Yes	Li-6	1.6	25.520	2	26	26.0	746.34	NE213-B	1.6	176	129.00	479.00	102606	300606176	UCRL-ID-131461
DM009	7Li0.5a	Yes	Li-7	0.5	8.970	4	30	38.8877	765.2	Pilot B	1.6	140	131.00	409.00	5	------	UCRL-51144
DM010	7Li0.5b	Yes	Li-7	0.5	8.970	4	120	116.7050	977.2	NE213-A	1.6	162	185.00	507.00	6	------	UCRL-51144
DM011	7Li0.5c	Yes	Li-7	0.5	8.970	2	26	26.0	746.34	NE213-B	1.6	172	129.00	471.00	102507	300702176	UCRL-ID-131461
DM012	7Li1.0a	No	Li-7	1.0	16.520	4	30	38.8877	765.2	Pilot B	1.6	138	135.00	409.00	7	------	UCRL-51144
DM013	7Li1.0b	No	Li-7	1.0	16.520	2	26	26.0	746.34	NE213-B	1.6	176	129.00	479.00	102509	------	-------
DM014	7Li1.0c	No	Li-7	1.0	16.520	2	26	26.0	878.0	Stilbene	0.8	370	149.00	887.00	------	300704180	UCRL-ID-131461
DM015	7Li1.6a	Yes	Li-7	1.6	25.520	4	30	38.8877	765.2	Pilot B	1.6	137	137.00	409.00	8	------	UCRL-51144
DM016	7Li1.6b	Yes	Li-7	1.6	25.520	2	26	26.0	746.34	NE213-B	1.6	176	129.00	479.00	102603	300706176	UCRL-ID-131461
•																	
•																	
•																	
DM155	Lwt1.1a	Yes	LWtr	1.1	10.480	5	30	38.8877	754.0	Pilot B	1.6	136	138.00	408.00	39	------	UCRL-51144
DM156	Lwt1.1b	Yes	LWtr	1.1	10.480	2	26	26.0	731.52	NE213-B	1.6	156	127.00	437.00	21816	131804171	UCRL-ID-131461
DM158	Lwt1.9a	Yes	LWtr	1.9	19.050	5	30	38.8877	754.0	Pilot B	1.6	134	132.00	398.00	40	------	UCRL-51144
DM159	Lwt1.9b	Yes	LWtr	1.9	19.050	3	120	116.7050	975.4	NE213-A	1.6	153	185.00	489.00	41	------	UCRL-51144
DM160	Lwt1.9c	Yes	LWtr	1.9	19.050	2	26	26.0	731.52	NE213-B	1.6	154	127.00	433.00	21812	------	-------
DM161	Lwt1.9d	Yes	LWtr	1.9	19.050	2	26	26.0	879.48	Stilbene	0.8	298	161.00	755.00	------	131808177	UCRL-ID-131461

1) This table only contains information on the 145 detector measurements (DMxxx) in the final Master Library for high-energy measurements. Originally, there were 161 entries but: 2 were redundant entries, 2 were non-traceable, and 12 were moved to a similar library for low-energy measurements.
2) In those cases where experimental data existed on both the "ExptData" and "Disp93in" data tapes, the original ID number of the recommended dataset finally adopted in this Master Library is underlined. Notes of explanation are included in the DMxxx.doc files in the "TextFILS" subdirectory.

A Typical DMxxx "Data File"

CASE (detector measurement number):	DM008
Material	Lithium-6
Expt. number in EXPTDATA:	102606
Expt. number in DISP93IN:	300606176
Outer radius (cm):	25.520
Size in mean free paths:	1.6
Pulse width, FWHM (ns):	2
Flightpath distance (cm):	746.34
Beamline used (name=appx deg):	26
Beamline angle relative to beam (deg):	26.0
Detector:	NE213-b
Detector bias:	1.6 MeV
Num. of data points:	176
Tmin (ns):	129.00
Tmax (ns):	479.00
Reference publication:	UCRL-ID-131461 (July 1998)
Additional comments & info:	See the DM008.TXT file

Time (ns)	Energy (MeV)	Counts/ns /source	Error	Integral
1.29000E+02	1.80020E+01	3.60647E-05	2.25525E-05	7.21294E-05
1.31000E+02	1.74410E+01	4.67088E-05	2.29053E-05	1.65547E-04
1.33000E+02	1.69060E+01	6.78181E-05	2.35896E-05	3.01183E-04
1.35000E+02	1.63960E+01	2.75105E-04	2.94765E-05	8.51393E-04
1.37000E+02	1.59090E+01	4.01199E-03	8.06267E-05	8.87537E-03
1.39000E+02	1.54430E+01	2.78635E-02	2.06026E-04	6.46023E-02
1.41000E+02	1.49970E+01	6.08930E-02	3.03686E-04	1.86388E-01
1.43000E+02	1.45710E+01	4.97472E-02	2.74641E-04	2.85883E-01
1.45000E+02	1.41630E+01	2.87324E-02	2.09180E-04	3.43347E-01
1.47000E+02	1.37720E+01	1.80378E-02	1.66249E-04	3.79423E-01
1.49000E+02	1.33960E+01	1.33934E-02	1.43664E-04	4.06210E-01
1.51000E+02	1.30370E+01	1.01401E-02	1.25444E-04	4.26490E-01

•
•
•

$$E = m_0\left[\frac{1}{\sqrt{1-\alpha^2}} - 1\right] = \text{neutron energy in "MeV"} \quad \text{where}$$

$$\alpha = d/(tc)$$

or

$$t = \left(\frac{d}{c}\right)\left[\frac{1}{\sqrt{1-\beta^2}}\right] = \text{time in "nanoseconds"} \quad \text{where}$$

$\beta = m_0/(m_0 + E)$ where m_0 = rest mass energy of neutron

A Typical DMxxx.DOC "Text File"

```
CASE (detector measurement number):                              DM008
-------------------------------------------------------------------------
Material                                                      Lithium-6
Expt. number in EXPTDATA:                                        102606
Expt. number in DISP93IN:                                     300606176
Outer radius (cm):                                               25.520
Size in mean free paths:                                            1.6
Pulse width, FWHM (ns):                                               2
Flightpath distance (cm):                                        746.34
Beamline used (name=appx deg):                                       26
Beamline angle relative to beam (deg):                             26.0
Detector:                                                      NE213-b
Detector bias:                                                 1.6 MeV
Num. of data points:                                               176
Tmin (ns):                                                      129.00
Tmax (ns):                                                      479.00
Reference publication:                  UCRL-ID-131461 (July 1998)
-------------------------------------------------------------------------

             DM008.TXT (comments and supplemental information)
-------------------------------------------------------------------------------
COMMENTS ON THE EXPERIMENTAL DATA:

1) Reference count rate data taken from dataset 102606 of EXPTDATA file.

   Data in DISP93IN had 125 time bins between 135 and 383 ns, while
   data in EXPTDATA had 176 time bins between 129 and 479 ns.  Results
   in both files were found to match identically at all measurement times
   they had in common, and the dataset in the EXPTDATA file was selected
   as the reference dataset because it covered a broader range of times.

2) While headers in both the EXPTDATA and DISP93IN files said beamline 26
   was used, DISP93IN "also" had iang=30 for some unknown reason.

COMMENTS ON THE MCNP MODEL:
MCNP input file:                                  6Li1.6b (alias DM008.i)
Status of model:                                     available & working
------------------------------
DM008:  Li-6,  1.6 mfp, fwhm=2.0 ns, NE213-B bias=1.6, FP=746.34 cm,  26-deg
------------------------------
Orig Ref/Figure:  See page 57 of "Livermore Pulsed Sphere Program:  Program
                  Summary Through July 1971", UCRL-51144, Rev I (Feb 10 1972)

Some Orig Specs:  Mass(Li) = 30351.0 grams (dist over 6 zones)
                  Mass(Stl)= 19014.0 grams (dist over 5 zones)
                  Matl densities: (not given)

Special note for the 6Li1.6 case:

This model preserves ALL the key dimensions of the configuration that are
explicitly shown on pp 57 of UCRL-51144.  This includes the outer radius
of all three (steel-cladded-lithium) spherical regions comprising the
experimental configuration, as well as explicit dimensions that are given
for the target cup nose cone.  The unmarked dimensions (such as the many
lithium-steel interfaces), however, must be based on those dimensions
+/- the thickness of the steel clad.  The figure on pp 57 of UCRL-51144
  •
  •  (continues for several pages)
  •
```

Marchetti's New "Collimated" Models

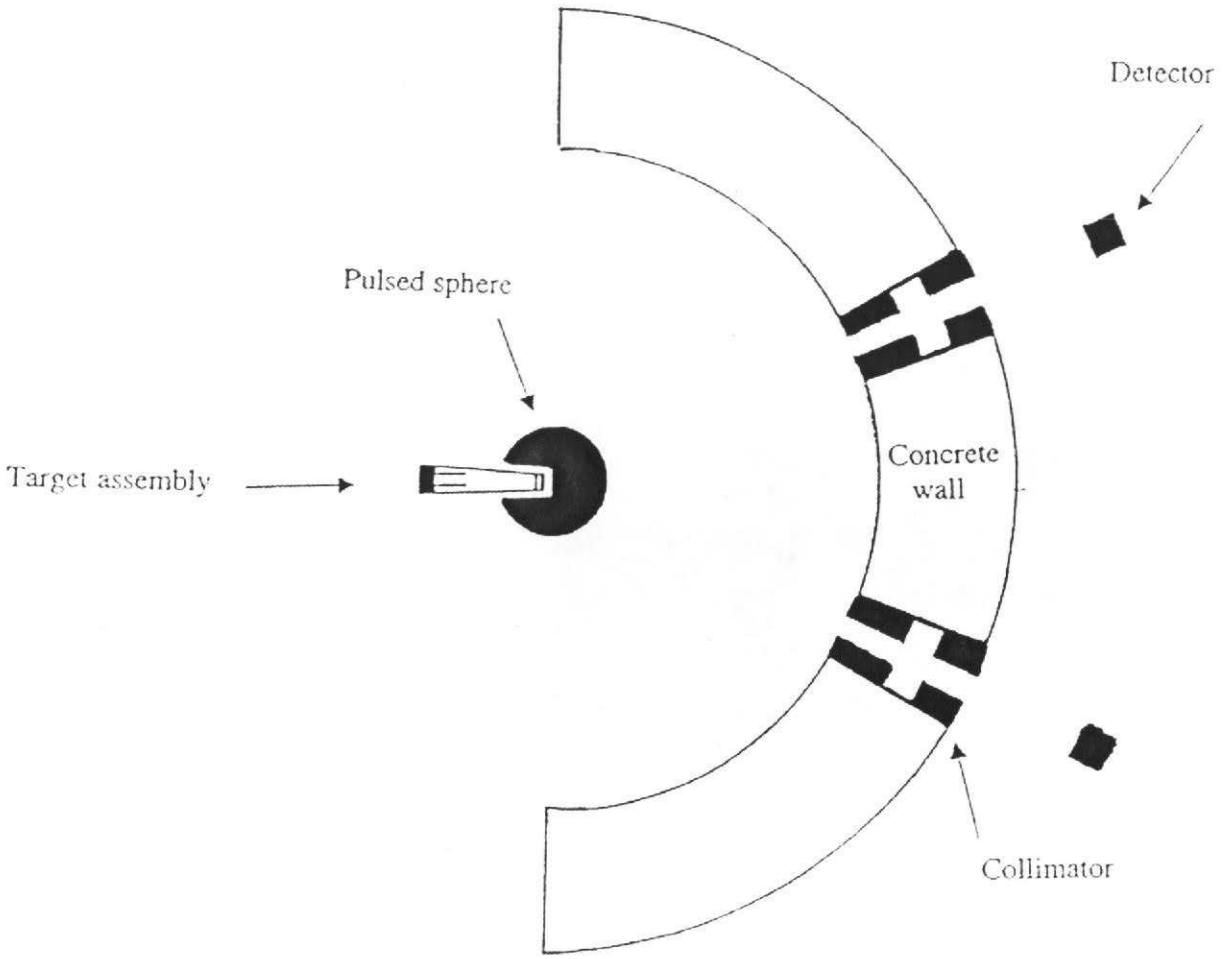

Fig. 5. Collimated detector model used by Marchetti in 1997. Taken from page 5 of UCRL-ID-131461.

Spark Renewed Interest in Pulsed Spheres

- High-energy results (10-12 MeV) differ from the earlier uncollimated results used to adjust ENDL data
- ENDF data may not be as good as previously thought

Our "Generic" MCNP Models

Used for Various Parametric Calculations

Typical Pulsed Sphere with Target Assembly Included

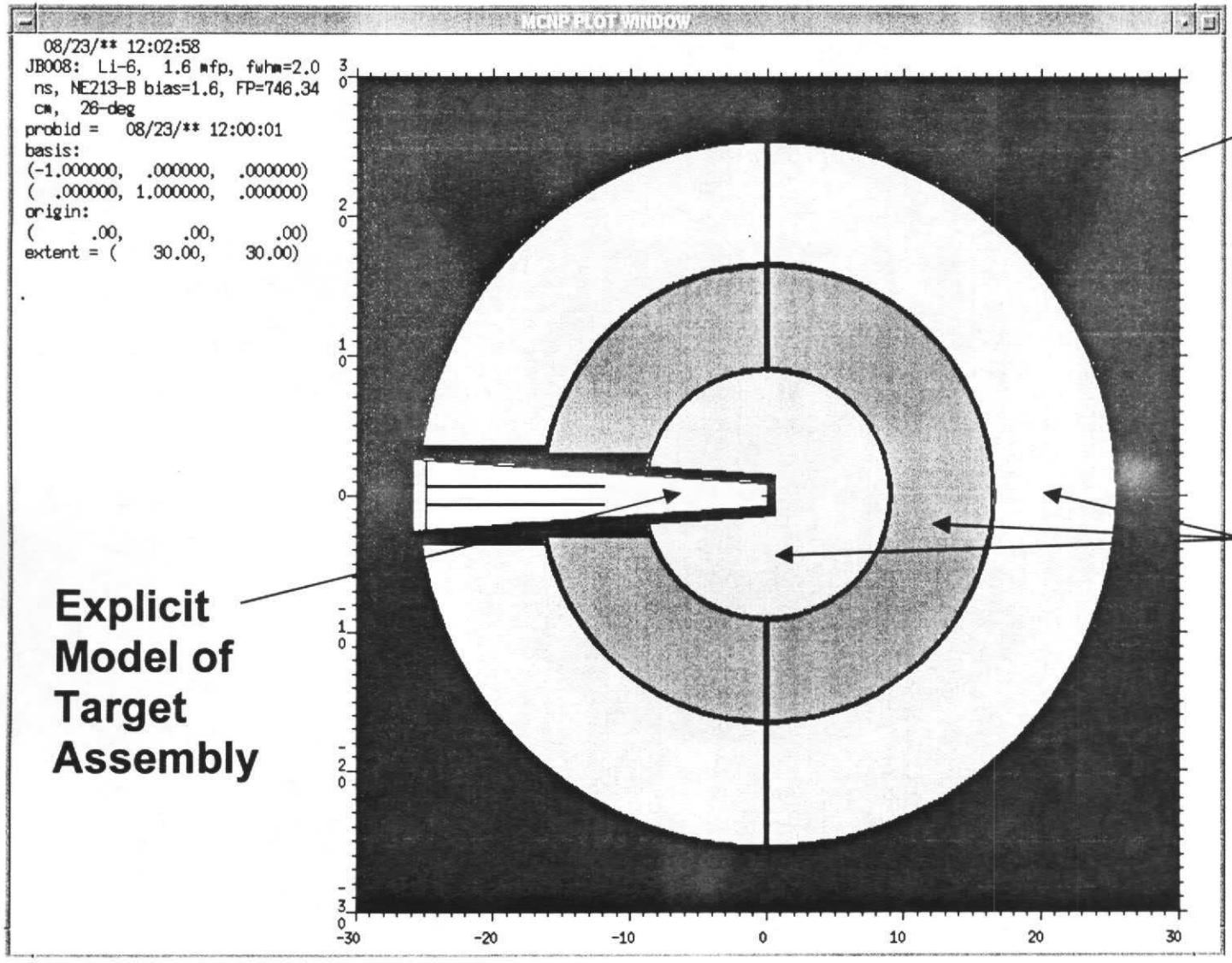

Overview of Sphere, Vault, and All 3 Beamlines

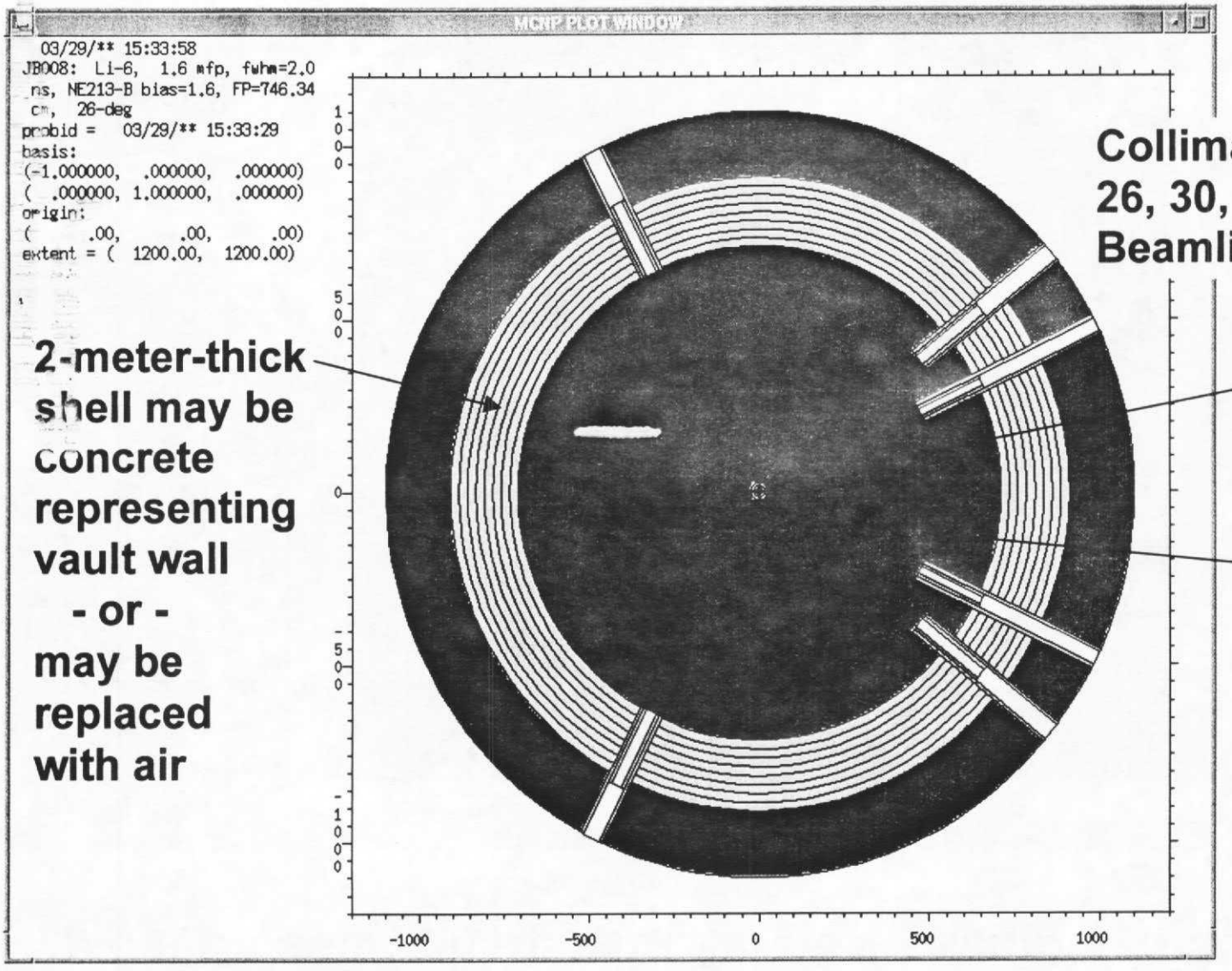

Features of the Generic Model

- Collimators may be treated as concrete or as neutronically black absorbers (imp:n=0)
- 2-meter-thick vault wall may be included, or ignored and replaced by air (made no noticable difference)
- Vault wall and collimators may be completely replaced by air to replicate the early uncollimated sea-of-air models (used before Marchetti)

Generic Model of a Collimator (vault wall not shown)

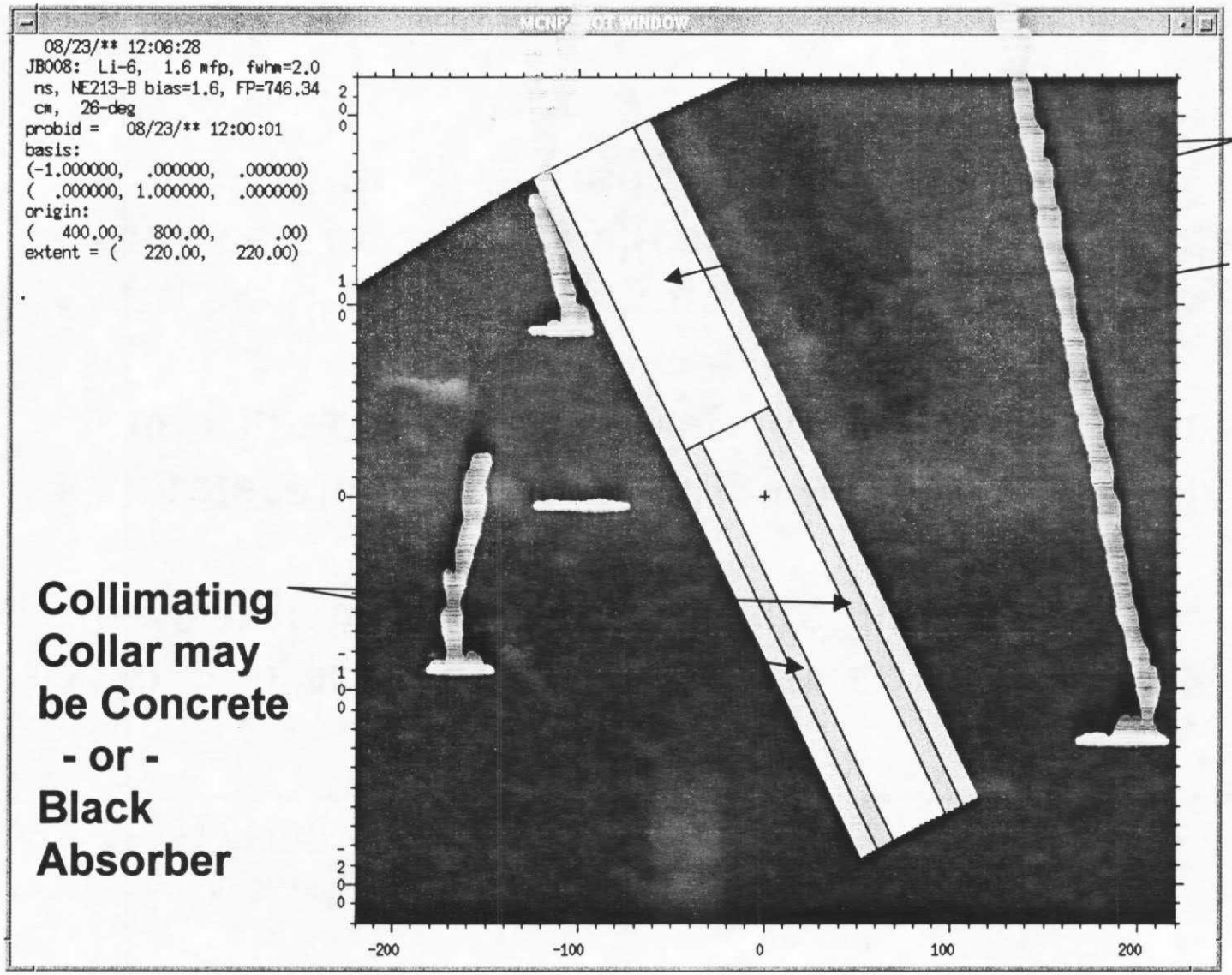

The Parametric Calculations

Part 1: to verify recent observations by others in a systematic fashion

Part 2: to evaluate proposed improvements of the MCNP models in a systematic fashion

Parametric Calcs – the suite of 13 test cases

- **Results always compared against the experimental measurements in this "test suite" which:**
- **Includes light, medium, and heavy spheres**
- **Includes large & small spheres of light material**
- **Includes fissile & non-fissile spheres**
- **Includes different detectors**
- **Includes measurements in all 3 beamtubes**

Detector Measurements Used for Evaluation Purposes:

```
DM002: 0.5 mfp Li-6 sphere      with NE213-A det at 120-deg
DM008: 1.6 mfp Li-6 sphere,     with NE213-B det at  26-deg
DM034: 0.9 mfp Aluminum sphere with NE213-A det at 120-deg
DM060: 0.5 mfp Carbon sphere    with NE213-A det at  30-deg
DM061: 0.5 mfp Carbon sphere,   with NE213-A det at 120-deg
DM080: 0.9 mfp Iron sphere      with NE213-B det at  30-deg
DM081: 0.9 mfp Iron sphere,     with NE213-A det at 120-deg
DM117: 0.7 mfp Pu-239 sphere,   with NE213-A det at  30-deg
DM118: 0.7 mfp Pu-239 sphere,   with NE213-A det at 120-deg
DM119: 0.7 mfp Pu-239 sphere,   with NE213-B det at  26-deg
DM136: 1.0 mfp Tungsten sphere with NE213-B det at  26-deg
DM142: 0.7 mfp U-235 sphere,    with NE213-B det at  26-deg
DM150: 0.8 mfp U-238 sphere,    with NE213-A det at 120-deg
```

Parametric Calcs – Results for Part 1

- Comparison plots show:

  Original uncollimated (sea-of-air) results
  vs Collimated results (without full concrete wall)
  vs Collimated results (with full concrete wall)
  vs Experimentally measured results

- Plots as a function of energy are more informative.

- More realistic collimated results are dramatically different from earlier sea-of-air results in 10.5-12.5 MeV energy range, especially for heavy spheres (whether fissile or non-fissile)

  -- Sea-of-air suffered unrealistic amt of skyshine
  -- More realistic collimated model compares less well with the actual experimental measurements
  -- Perhaps xsect data not as good as prev thought (?)

- Differences are far less noticeable /non-existent/ for light spheres – except maybe on 120 deg beamline (where they are still small).

- Adding the full concrete wall of the vault to the collimated model made virtually no difference (except to increase running time).

  -- Absolutely no differences seen when plotted as a function of time.

Pu-239 results vs Energy

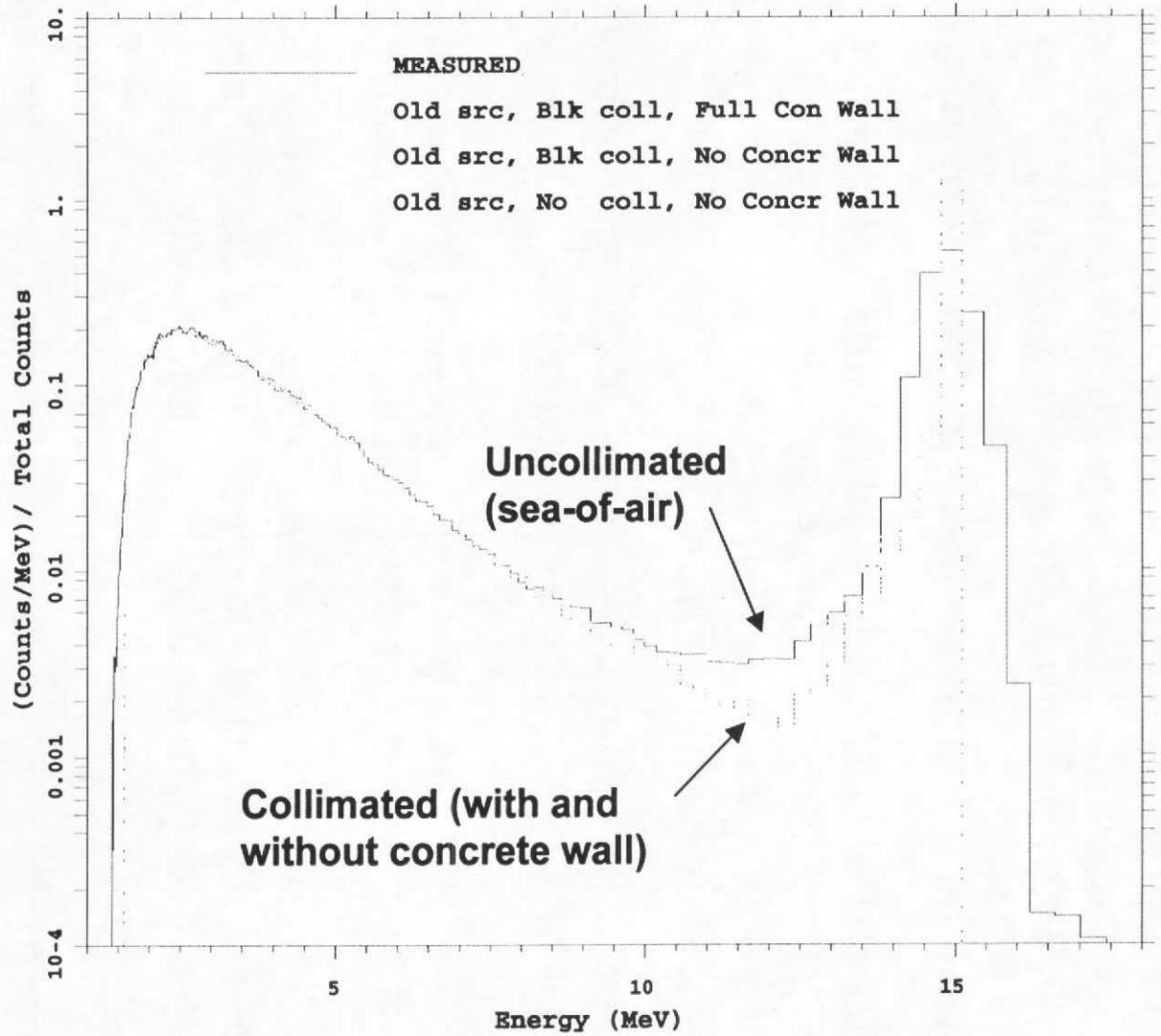

Fig. 28b. Comparison of results vs energy, with and without the full concrete wall, and with and without a collimator, but always with the traditional (old) source, for a 0.7 mfp Pu-239 sphere (DM119).

-- Wall therefore not included in final ref models.

Tungsten results vs Energy

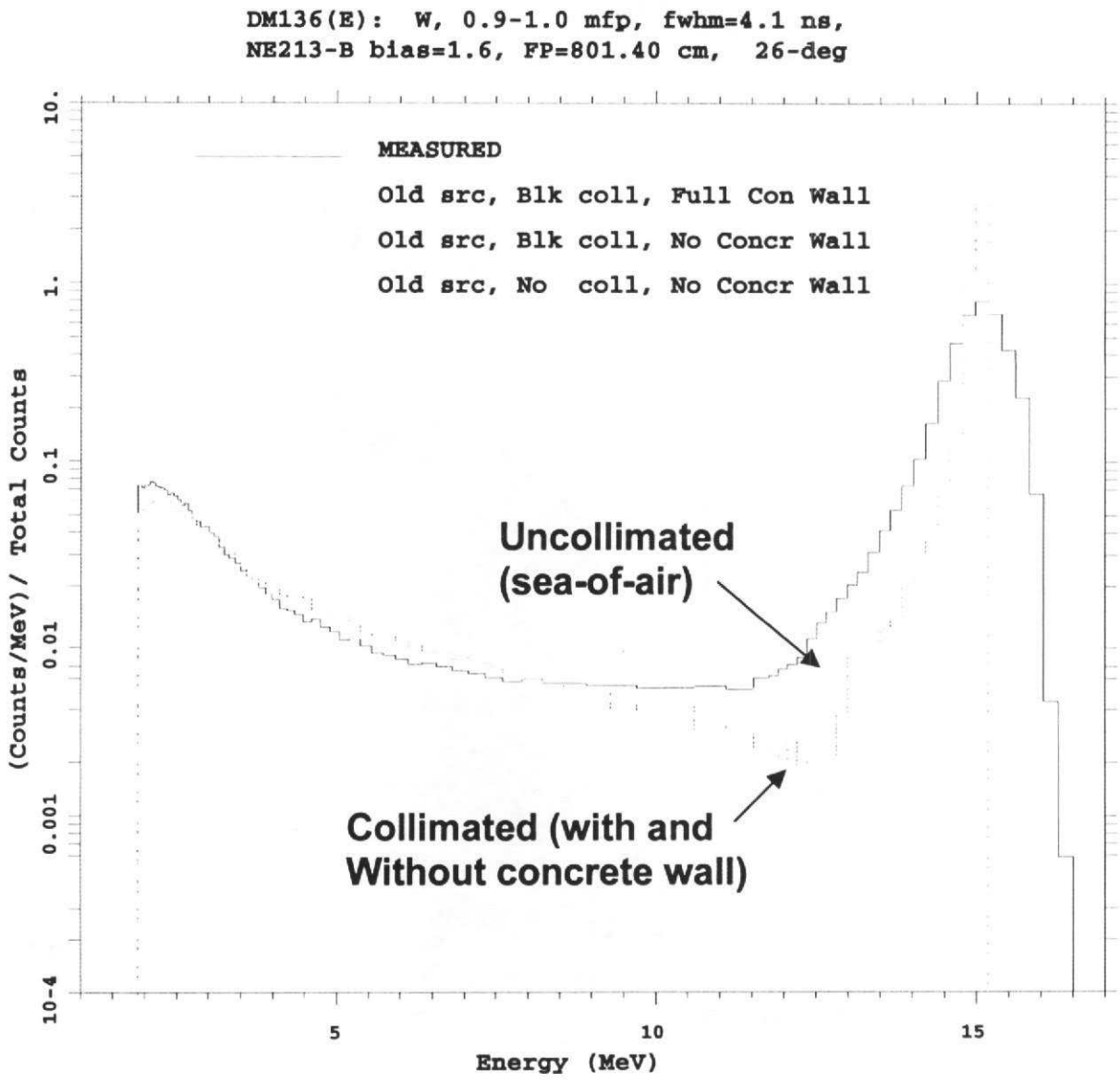

Fig. 29b. Comparison of results vs energy, with and without the full concrete wall, and with and without a collimator, but always with the traditional (old) source, for a 1.0 mfp Tungsten sphere (DM136).

Iron results vs Energy

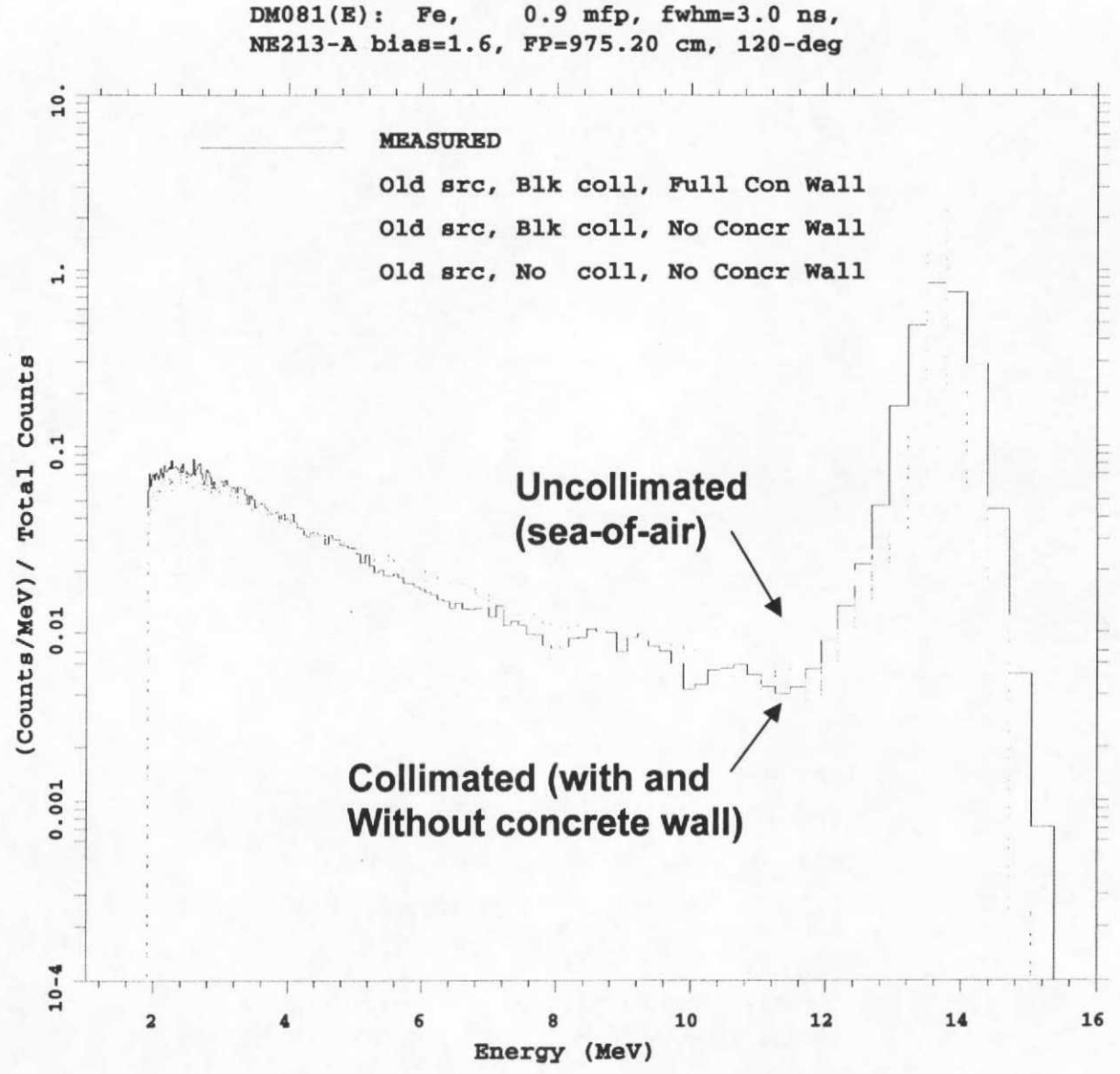

Fig. 26b. Comparison of results vs energy, with and without the full concrete wall, and with and without a collimator, but always with the traditional (old) source, for a 0.9 mfp Iron sphere (DM081).

Pu-239 results vs Time

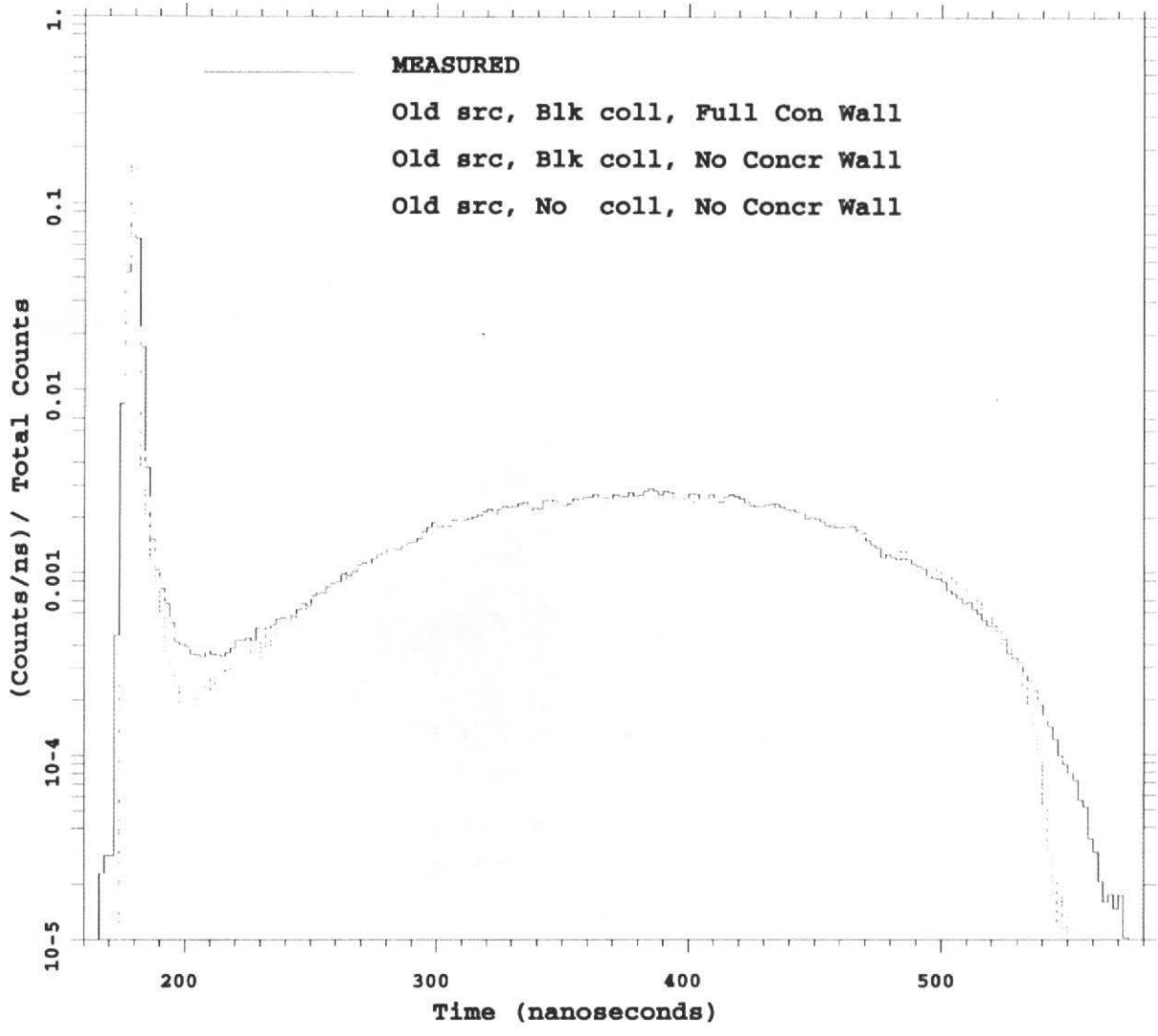

Fig. 28a. Comparison of results vs time, with and without the full concrete wall, and with and without a collimator, but always with the traditional (old) source, for a 0.7 mfp Pu-239 sphere (DM119).

Tungsten results vs Time

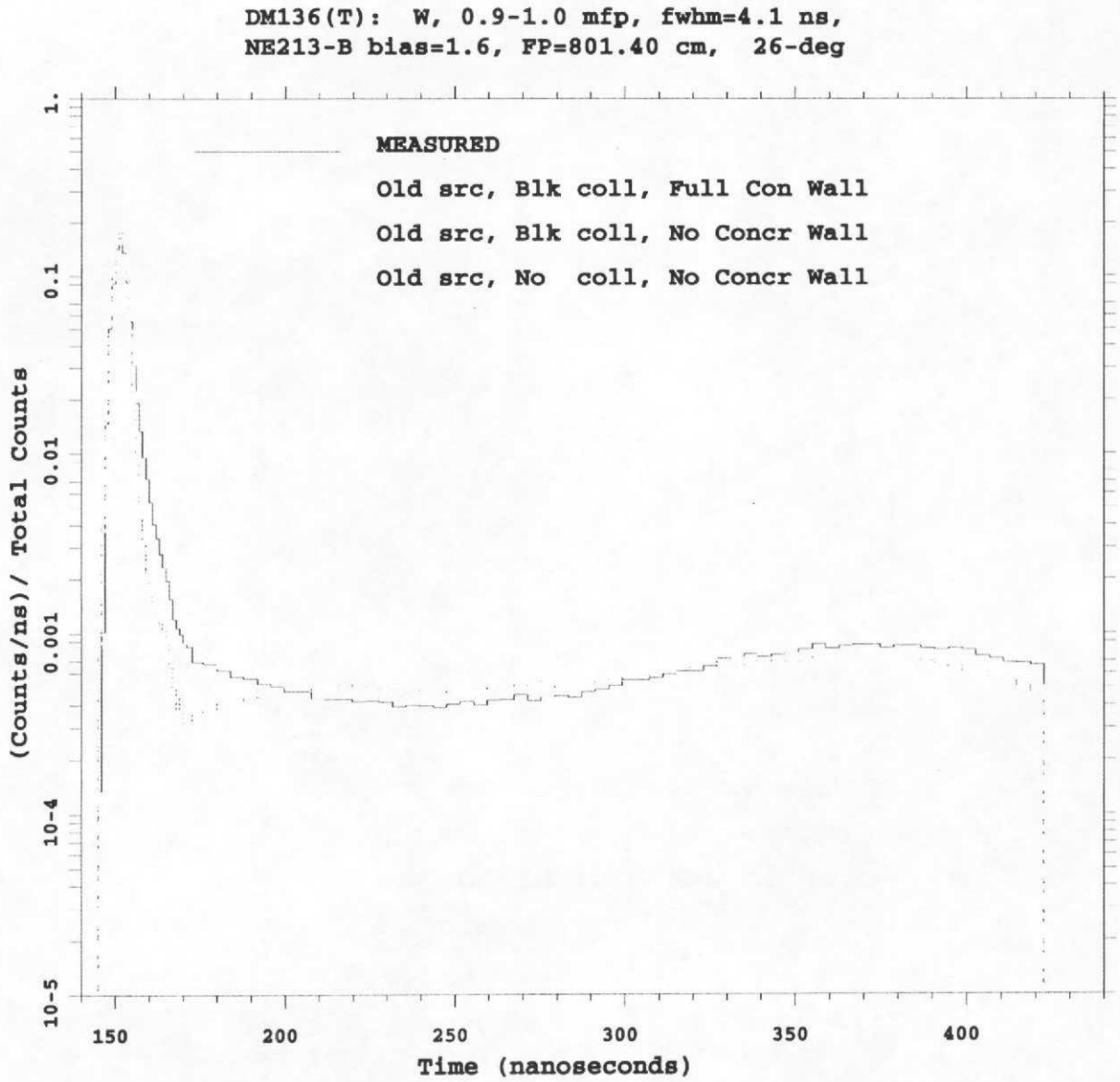

Fig. 29a. Comparison of results vs time, with and without the full concrete wall, and with and without a collimator, but always with the traditional (old) source, for a 1.0 mfp Tungsten sphere (DM136).

Iron results vs Time

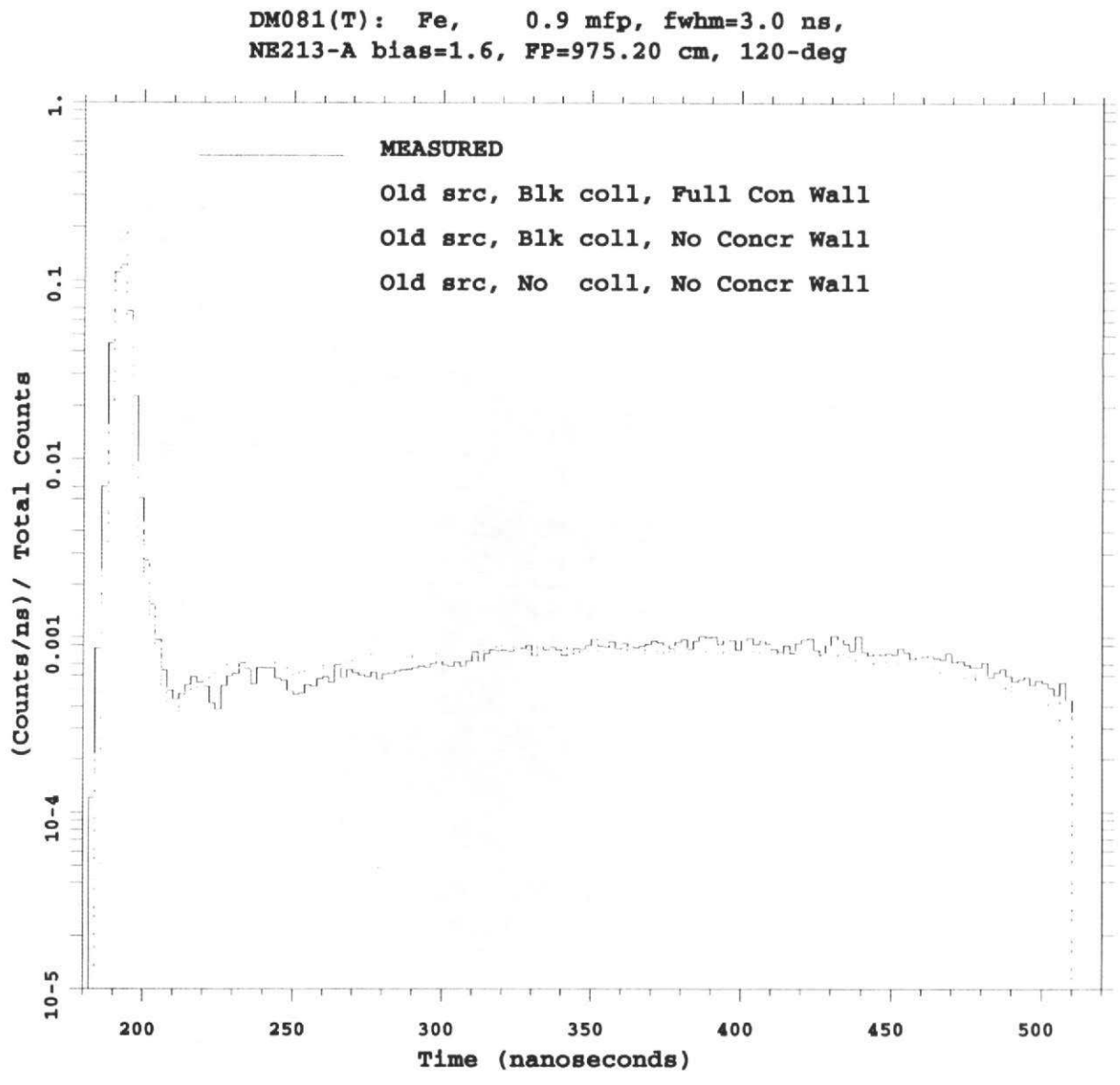

Fig. 26a. Comparison of results vs time, with and without the full concrete wall, and with and without a collimator, but always with the traditional (old) source, for a 0.9 mfp Iron sphere (DM081).

Parametric Calcs – Part 2

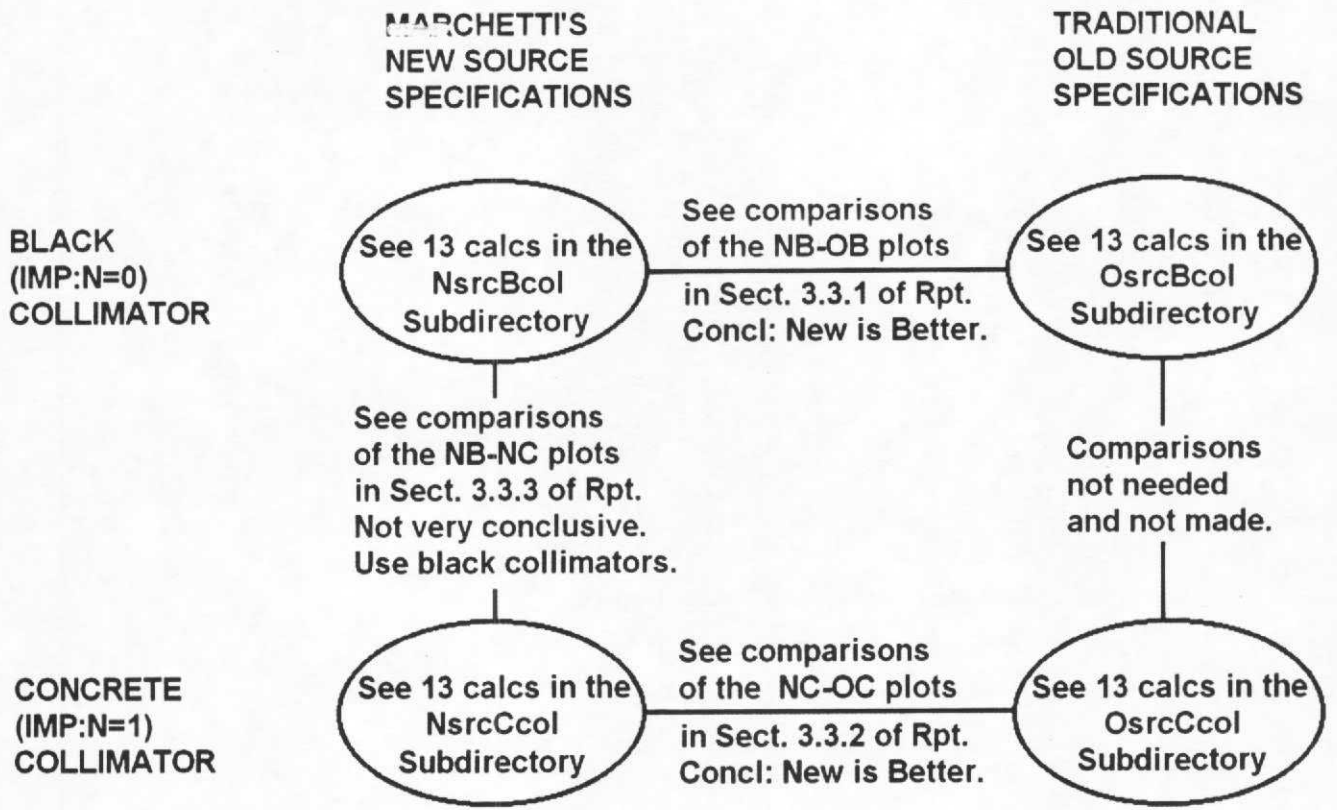

Fig. 32. New parametric calculations and comparisons to determine the best source terms and collimator models.

Parametric Calcs – Part 2a: New Source vs Old Source

- **Marchetti's new source has revised "space-energy-direction-dependent" specifications for neutrons from tritiated target that differ from the traditional (old) source terms.**
- **Generally found to yield "much better" results than old source in the 13-15 MeV energy range.**
- **Results "at least as good as" with old source at lower energies.**
- **Above conclusions were true whether we used collimators made of concrete or black absorbers.**
- **Marchetti's new source specs were therefore adopted as the new standard for the final reference calculations.**

New Source vs Old Source

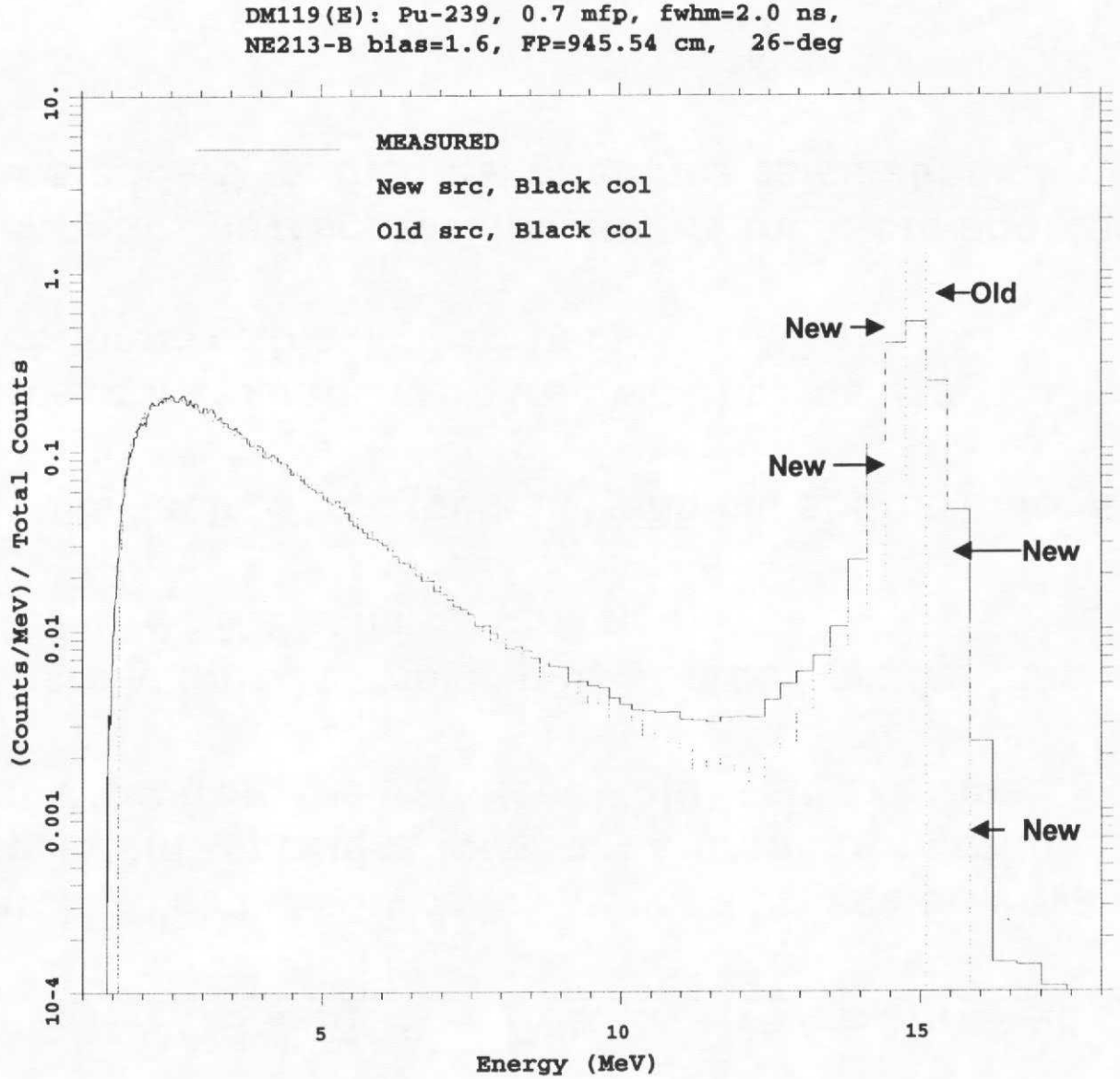

Fig. 36b. Comparison of results vs energy using the new source and the old source, both in conjunction with a black collimator, for a 0.7 mfp Pu-239 sphere (DM119).

New Source vs Old Soure

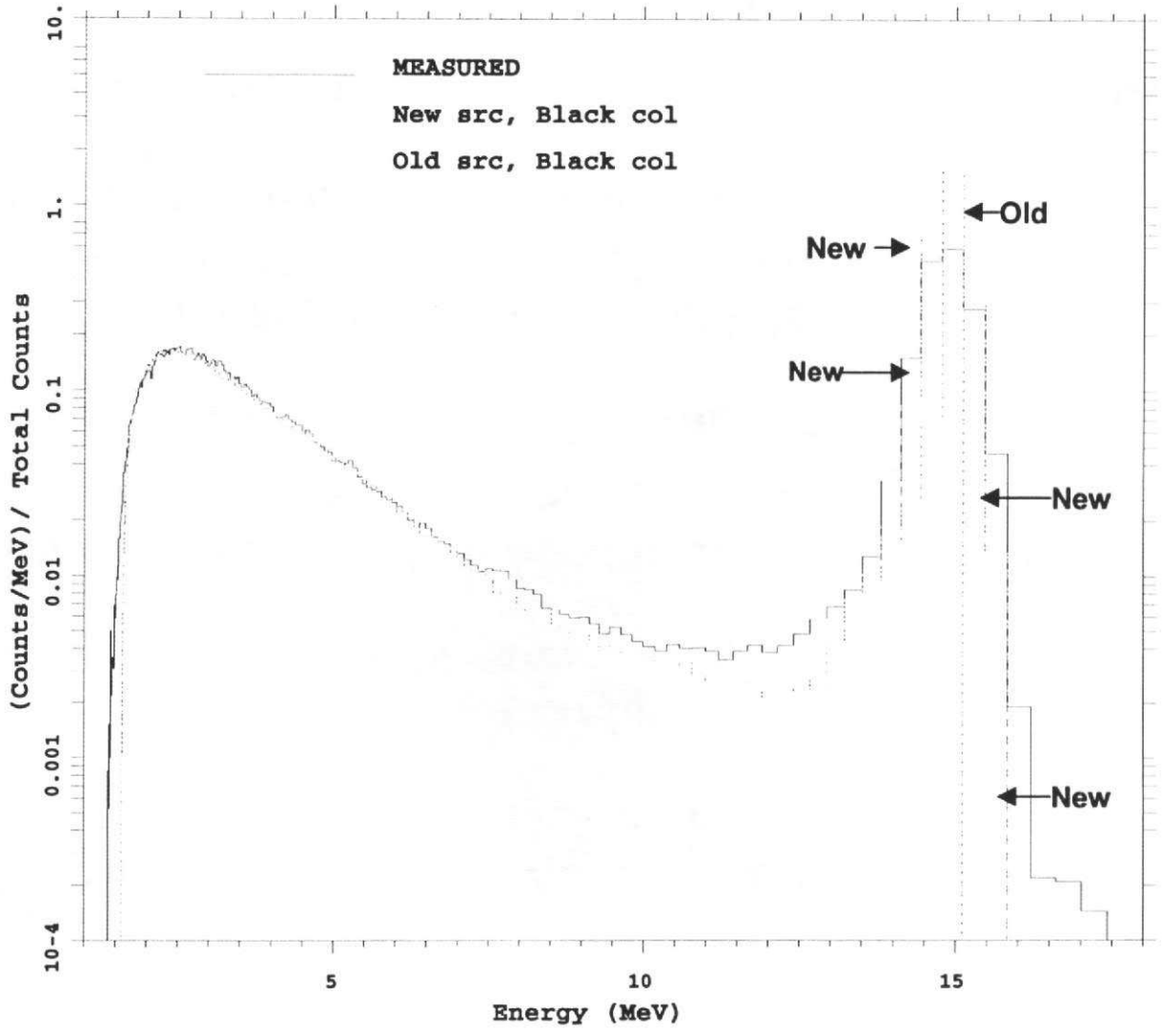

Fig. 37b. Comparison of results vs energy using the new source and the old source, both in conjunction with a black collimator, for a 0.7 mfp U-235 sphere (DM142).

Parametric Calcs – Part 2b: Type of Collimators (Blk vs Conc)

- Looked at representing the collimators in the beamtubes as real concrete vs neutronically black absorbers (imp:n=0)
- The hope was to better represent reflective and moderating effects "inside" the beamtube, closer to the detectors.
- Both are approximations when used in context of the present RZ-symmetric model with ring detectors; physics not represented well in either case (with this model). Will explain later.
- Differences in comparison plots were visible, but no firm conclusion could be drawn; black was better 55% of time; concrete was better 45%of time, but no clear pattern could be seen
- Final recommendation was to use black collimators (for now).
- In the future, true 3-D models with "cylindrical" beamtubes and DXTRAN spheres to better sample collisions in the concrete collimators may(?) improve results in 10.5 to 12.5 MeV region

Parametric Calcs – Part 2b: Type of Collimators (Details)

Comments apply to next 5 slides:

- **Sometimes the black collimator agreed better with experiments (see Fe sphere at 30 deg vs Time)**
- **Sometimes the black and concrete collimators gave roughly the same result (see U-235 sphere at 26 deg vs Time)**
- **Sometimes the concrete collimator agreed better with experiments (see Pu-239 at 120 deg vs Time)**
- **Sometime both collimator models appeared equally bad -- with concrete high, and black low (see Pu-239 at 30 deg vs Time)**
- **Sometimes you form one opinion when looking at results vs time (see Pu-239 at 30 deg vs Time) and a different opinion when looking at the same results vs energy (see Pu-239 at 30 deg vs Energy)**
- **No clear pattern could be identified.**

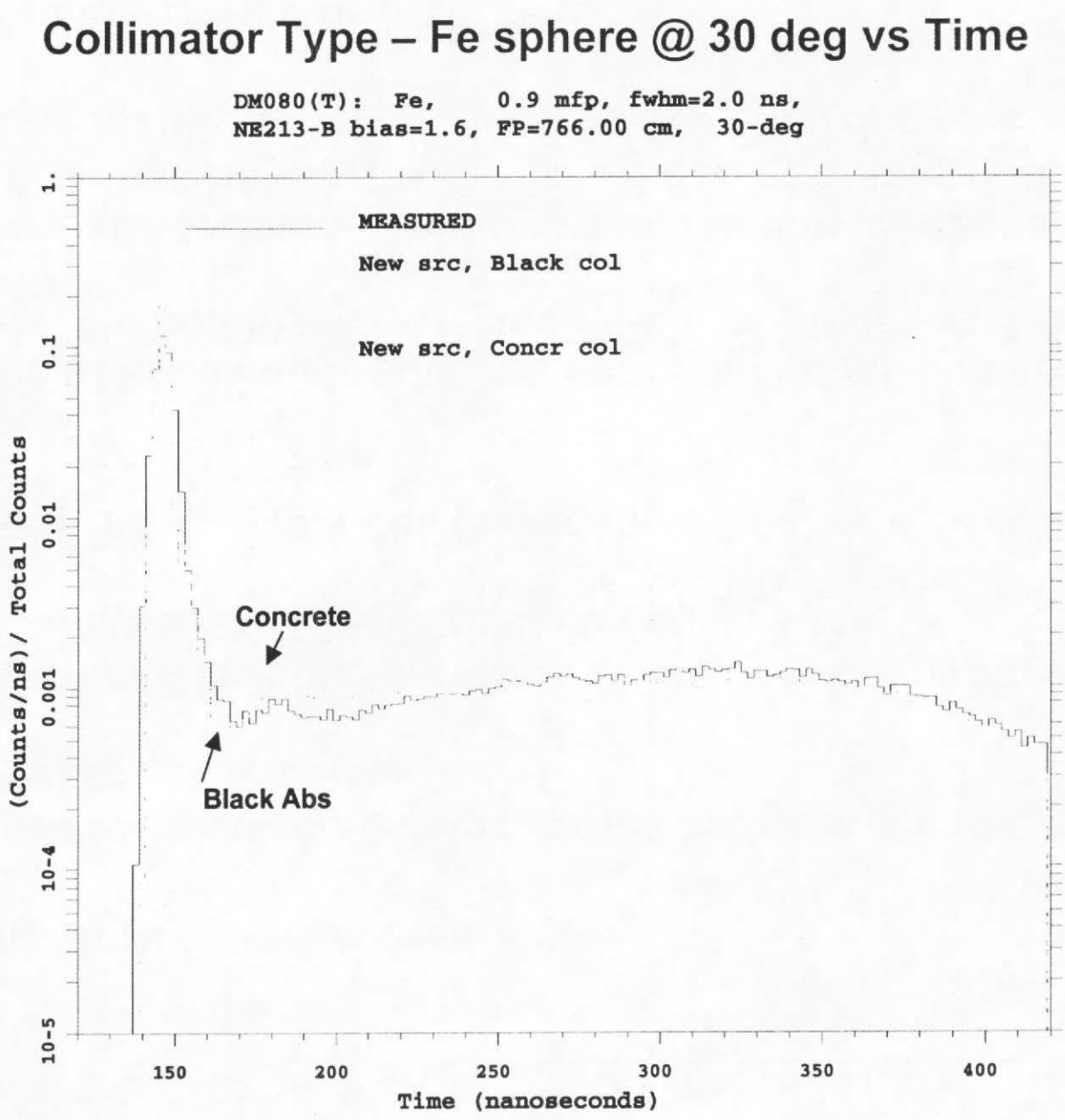

Fig. 39a. Comparison of results vs time using a black collimator and a concrete collimator, both in conjunction with Marchetti's new source, for a 0.9 mfp Iron sphere (DM080).

Collimator Type – U-235 sphere @ 26 deg vs Time

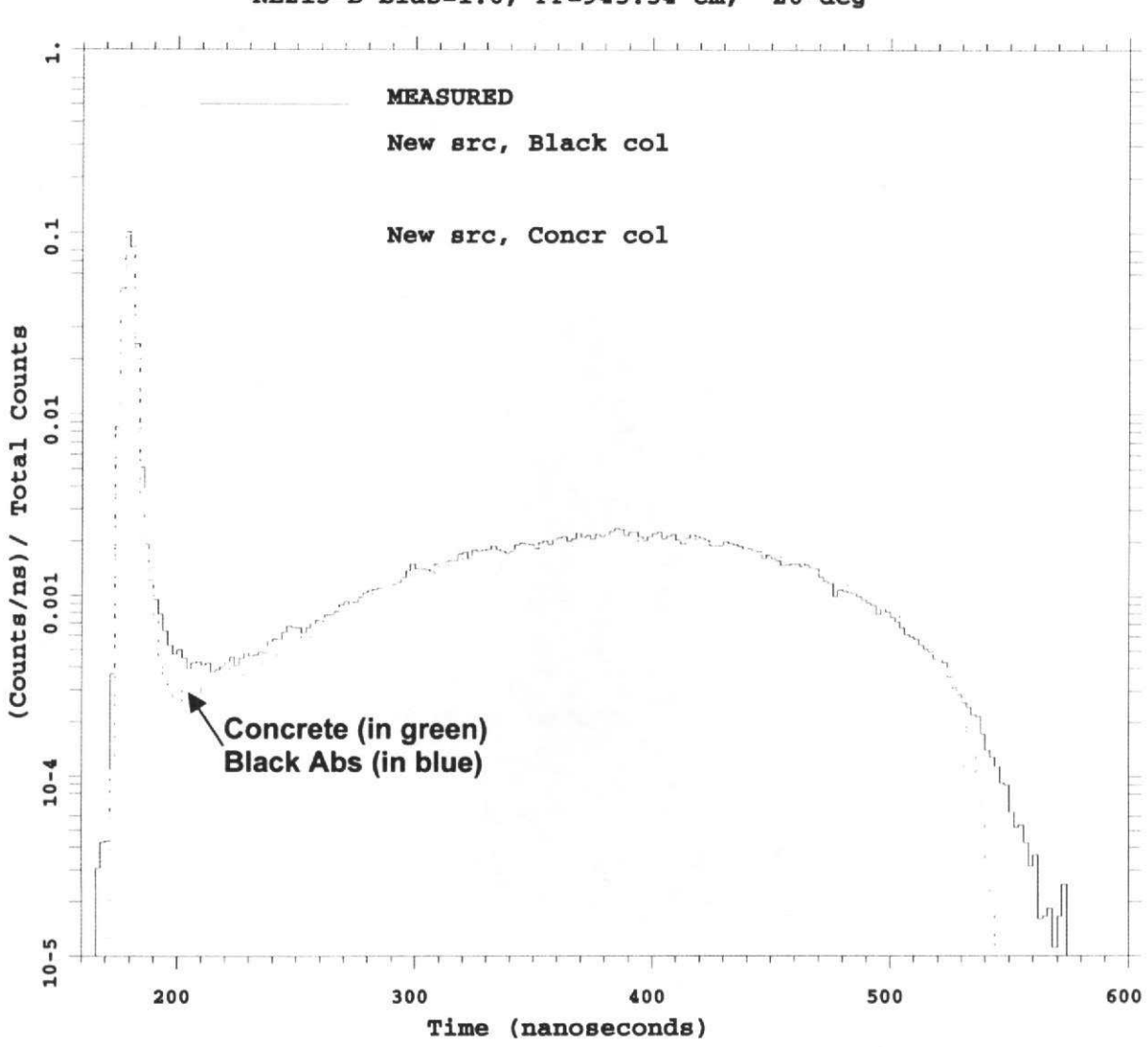

Fig. 42a. Comparison of results vs time using a black collimator and a concrete collimator, both in conjunction with Marchetti's new source, for a 0.7 mfp U-235 sphere (DM142).

Collimator Type – Pu-239 sphere @ 120 deg vs Time

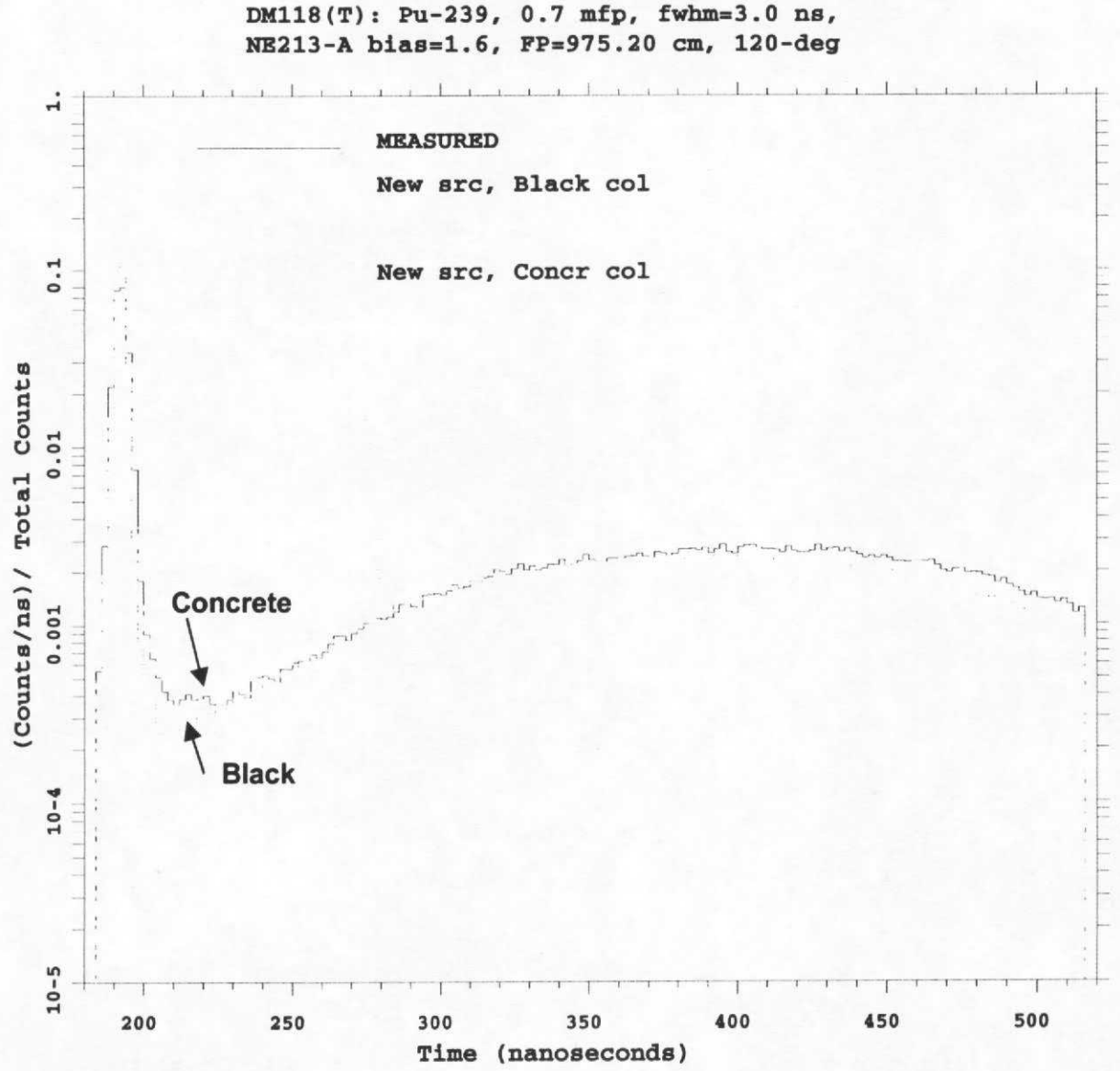

Fig. 41a. Comparison of results vs time using a black collimator and a concrete collimator, both in conjunction with Marchetti's new source, for a 0.7 mfp Pu-239 sphere (DM118).

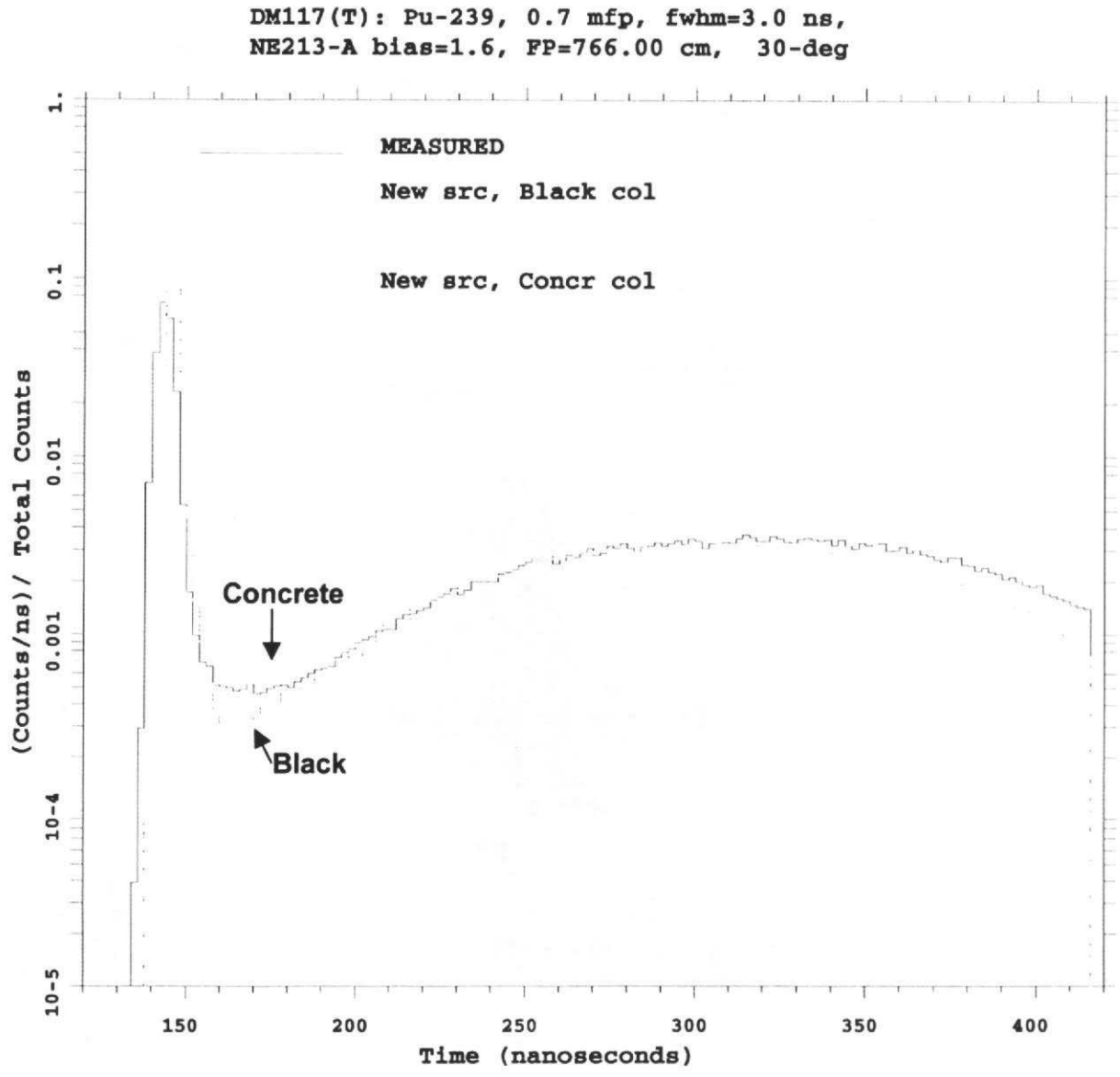

Fig. 40a. Comparison of results vs time using a black collimator and a concrete collimator, both in conjunction with Marchetti's new source, for a 0.7 mfp Pu-239 sphere (DM117).

Collimator Type – Pu-239 sphere @ 30 deg vs Energy

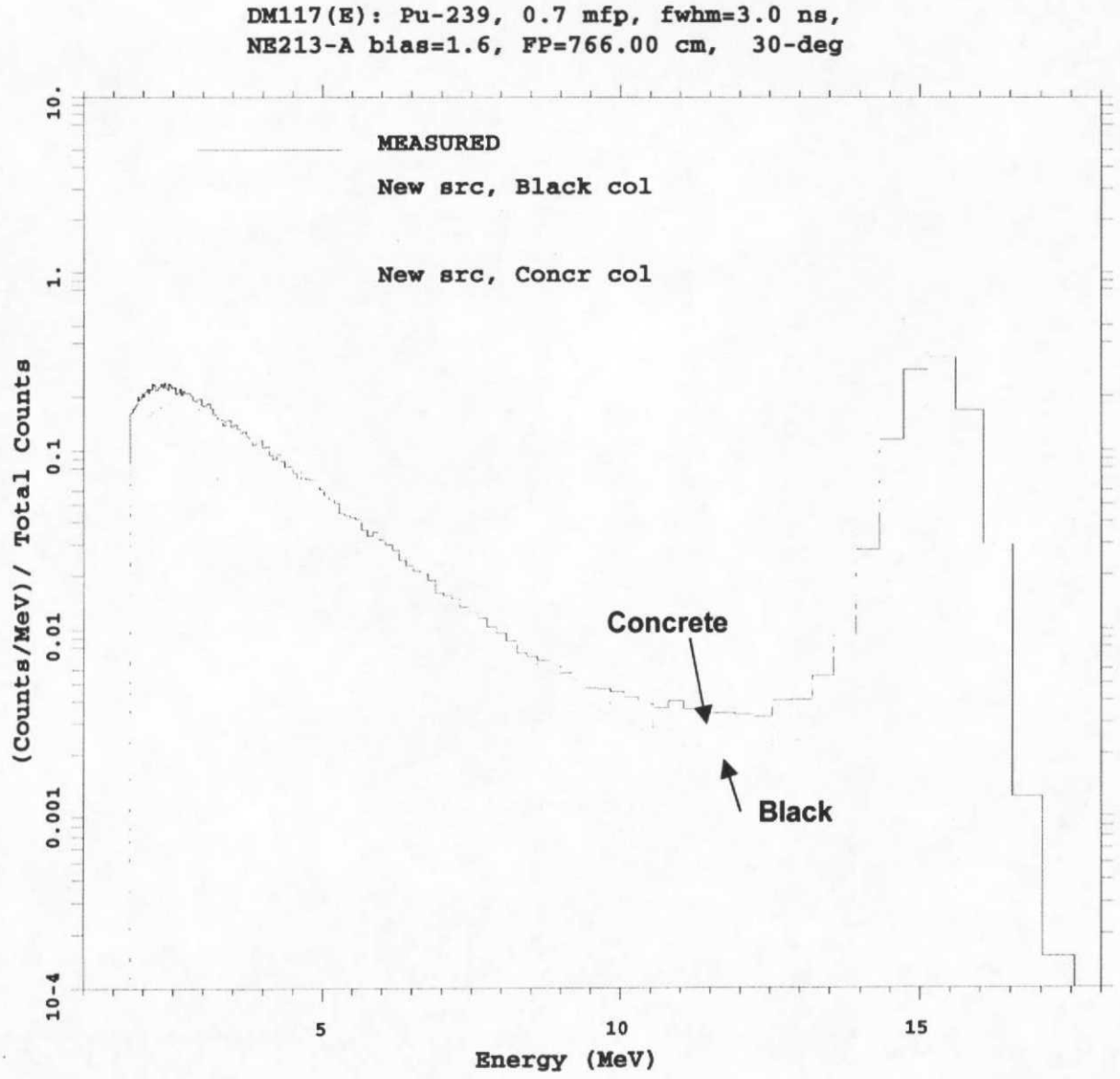

Fig. 40b. Comparison of results vs energy using a black collimator and a concrete collimator, both in conjunction with Marchetti's new source, for a 0.7 mfp Pu-239 sphere (DM117).

Parametric Calcs – Part 2b: Type of Collimators (Final)

- Differences in comparison plots were visible, but no firm conclusion could be drawn; black was better 55% of time; concrete was better 45% of time, but no clear pattern could be seen
- Final recommendation was to use black collimators (for now).
- In the future, true 3-D models with "cylindrical" beamtubes and DXTRAN spheres to better sample collisions in the concrete collimators may(?) improve results in 10.5 to 12.5 MeV region and/or resolve questions.

Final Reference Models and Calculations

comparing the ENDF60, ENDF66, and ENDL92 results against the experimental measurements

The Final Reference Models

- Always included explicit model of target assembly
- Used Marchetti's new source term specifications
- Treated the collimators as black absorbers
- Did not include the concrete wall of the vault

The Final Reference Calculations

- Were performed for 76 of the 145 detector measurements in the high-energy Master Library.
- This subset includes 36 of the 75 pulsed-sphere configurations in the Master Library
- and 20 of the 32 materials in the Master Library.
- All calcs were performed with 2,000,000 neutron histories
- All calcs were repeated using the ENDF60, ENDF66, and FNDLS2 cross-section libraries.
- Comparison plots show all these results, as well as measured results, as a function of time and as a function of energy.

Some Typical Comparison Plots vs Time

(Next 5 slides show: Pu-239, U-235, Fe, Li-6, Lwtr)

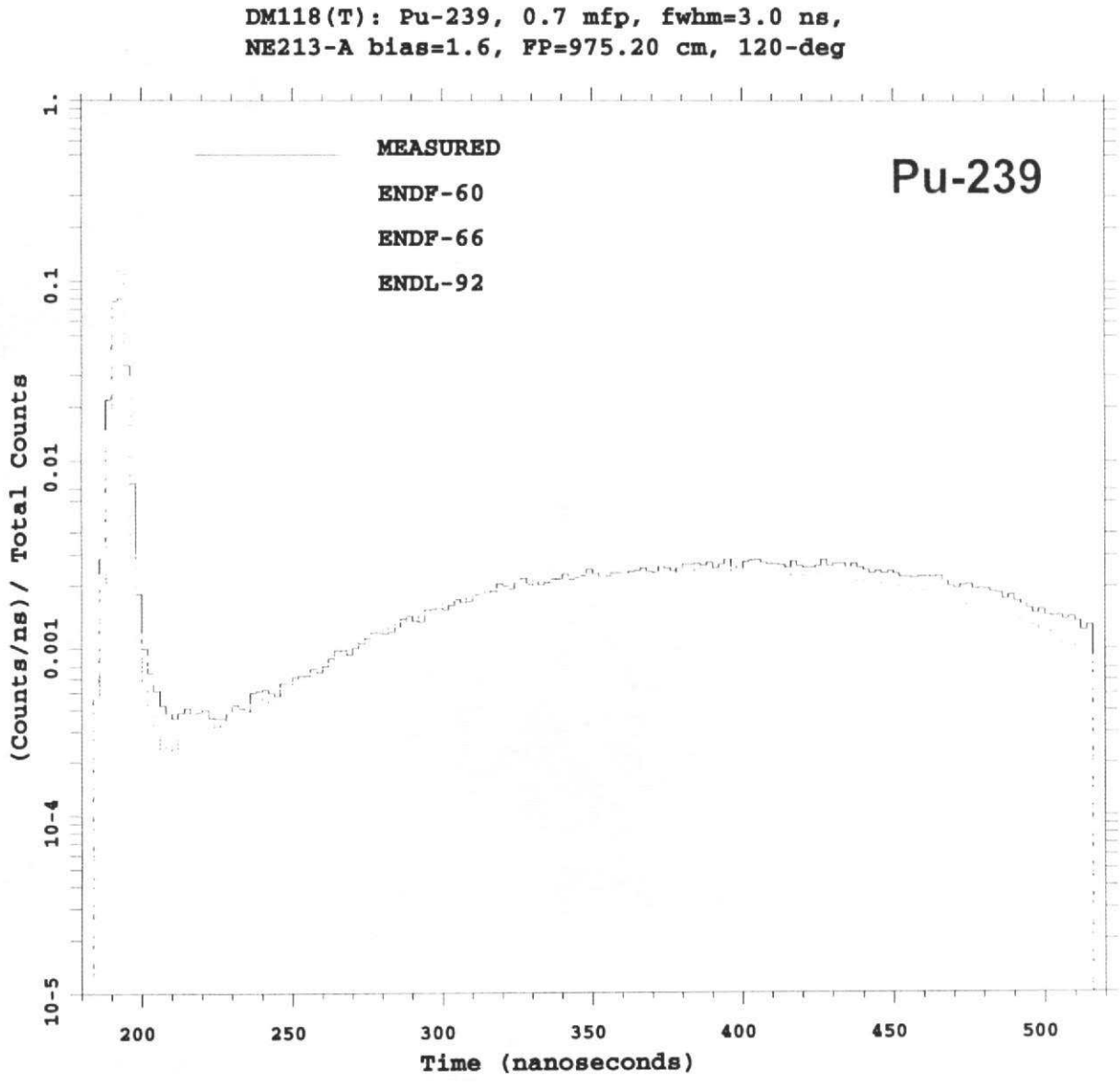

Fig. 55a. Comparison of results vs time for a 0.7 mfp Pu-239 sphere (DM118).

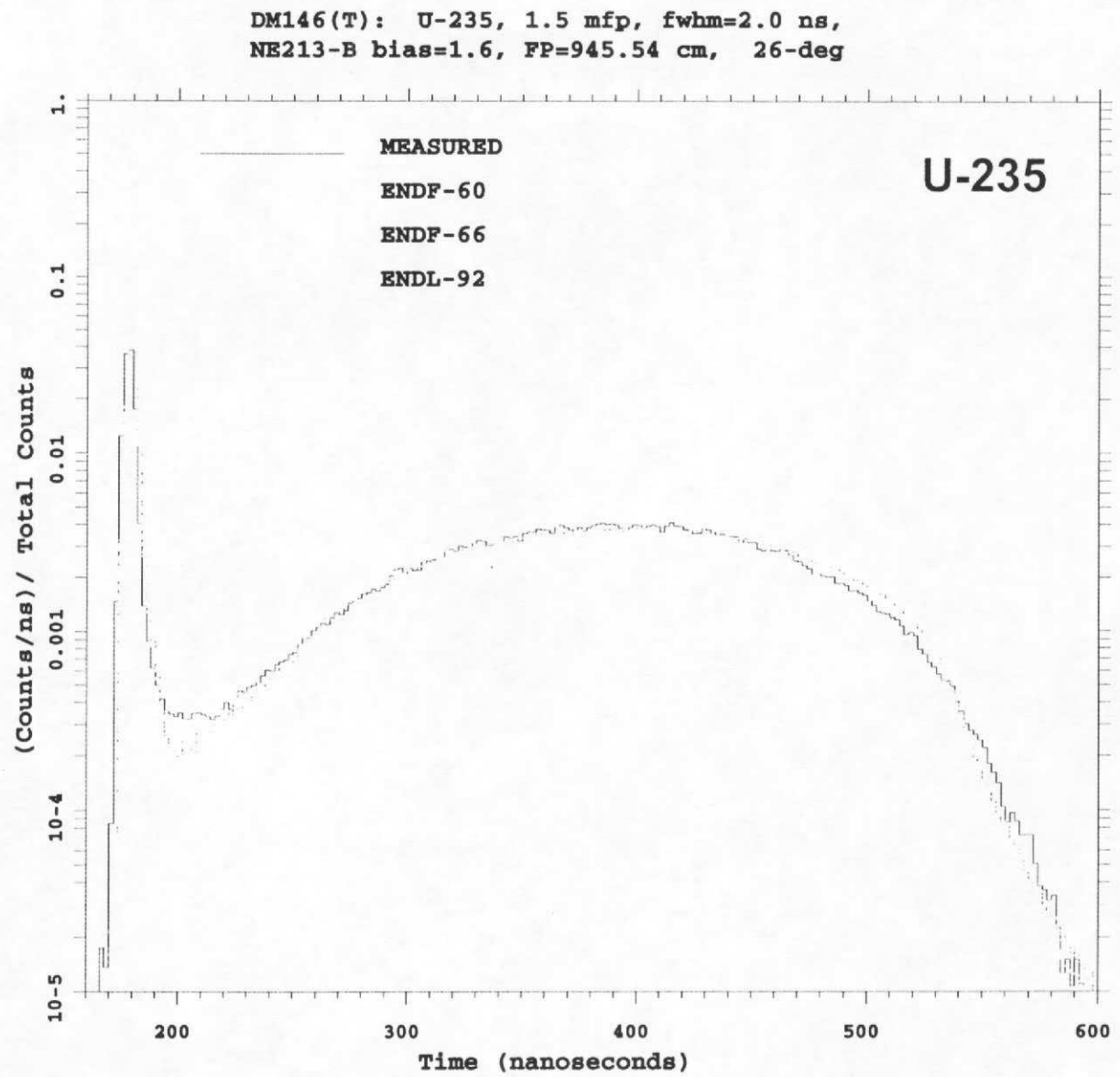

Fig. 59a. Comparison of results vs time for a 1.5 mfp U-235 sphere (DM146).

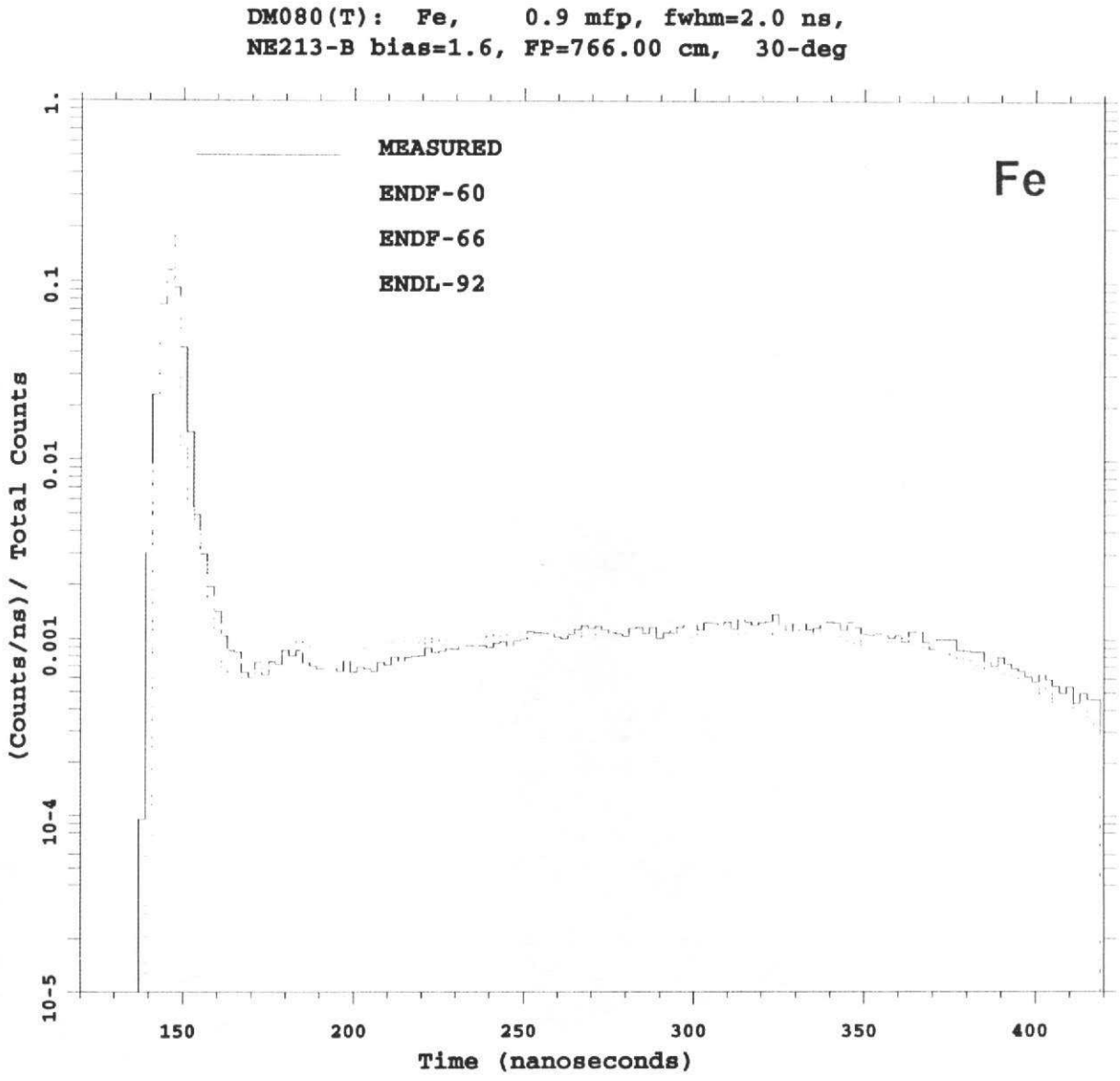

Fig. 50a. Comparison of results vs time for a 0.9 mfp Iron sphere (DM080).

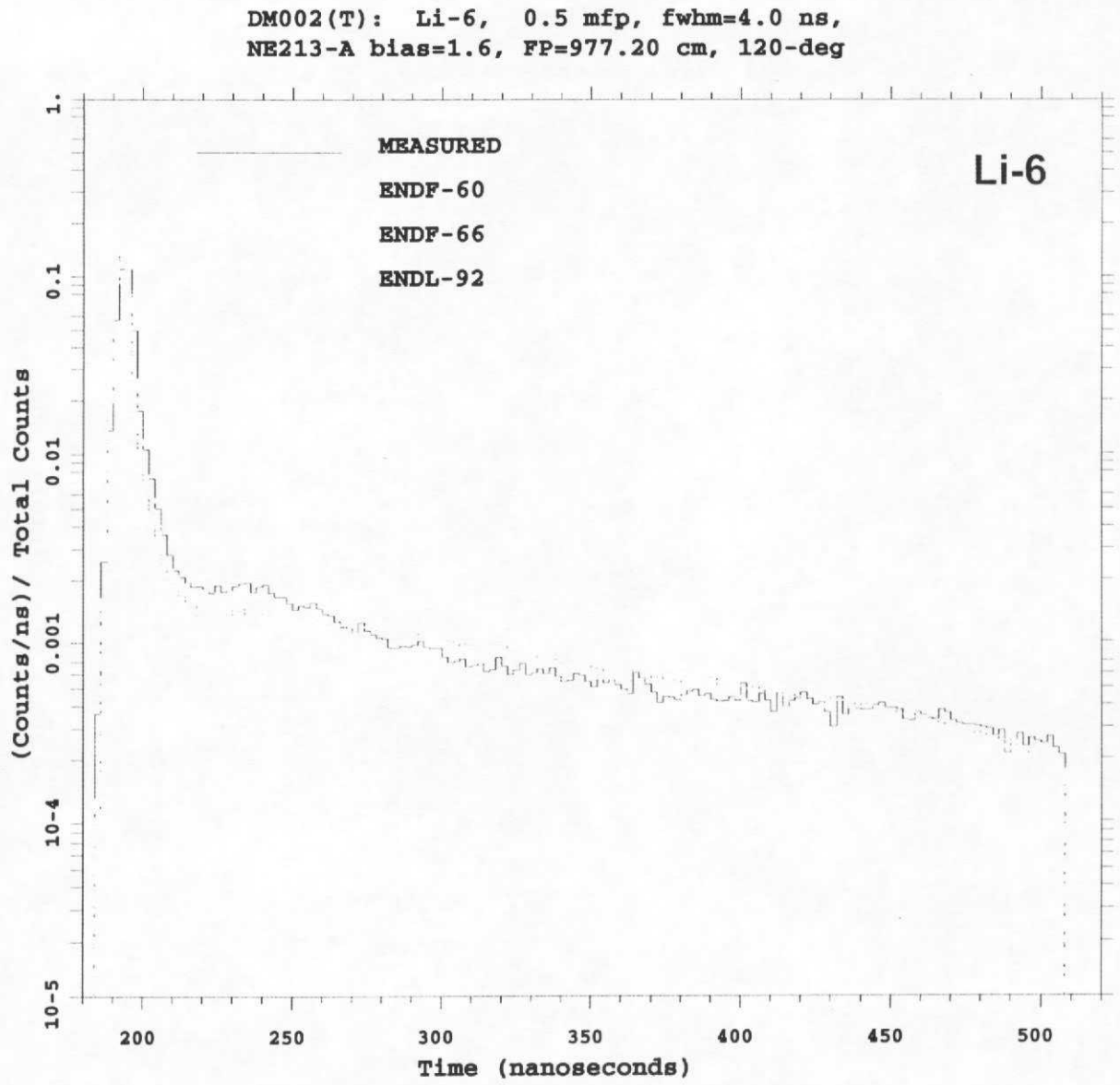

Fig. 43a. Comparison of results vs time for a 0.5 mfp Li-6 sphere (DM002).

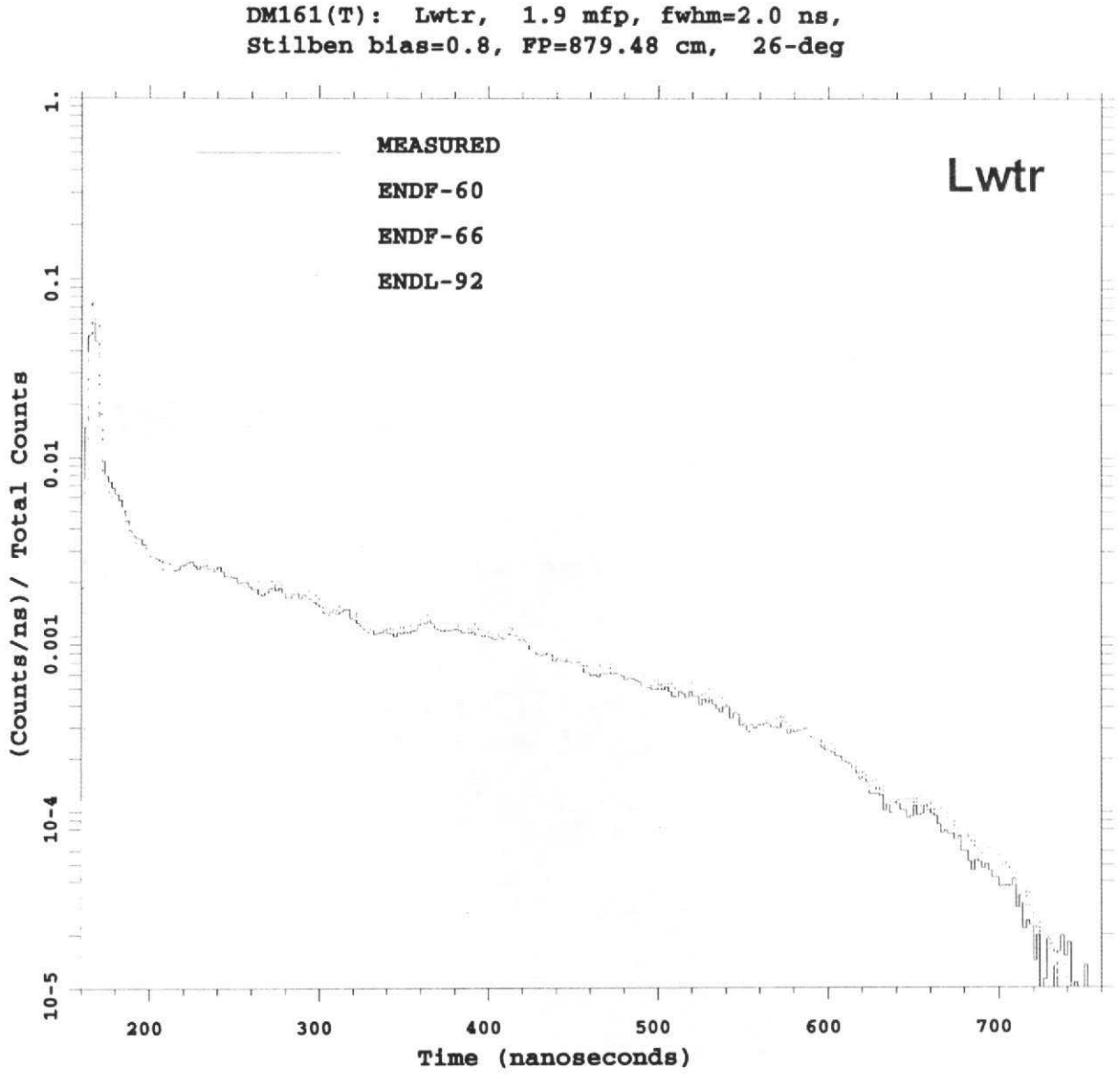

Fig. 62a. Comparison of results vs time for a 1.9 mfp Light Water sphere (DM161).

Same Typical Comparison Plots vs Energy

(Next 5 slides show: Pu-239, U-235, Fe, Li-6, Lwtr)

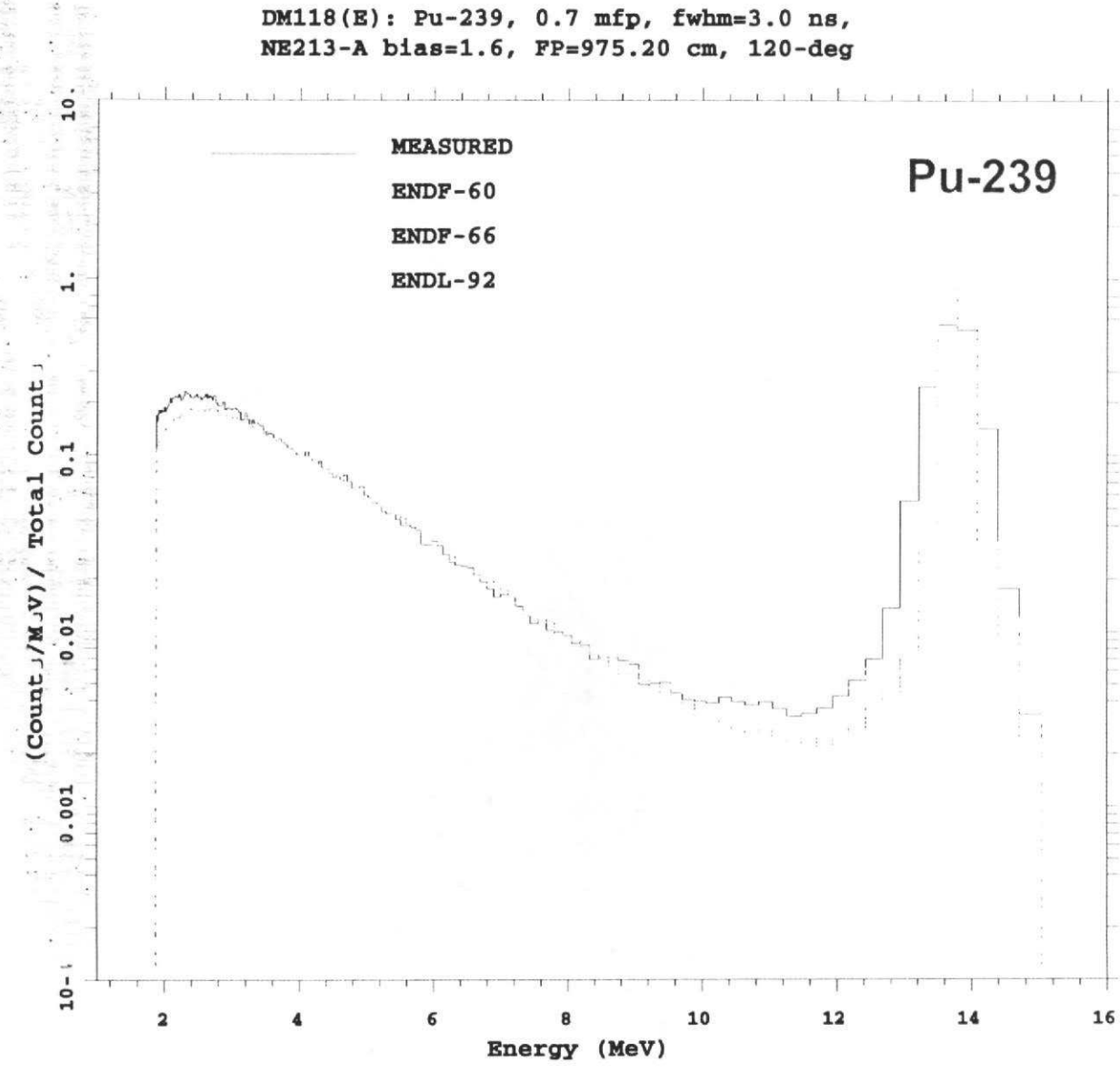

Fig. 55b. Comparison of results vs energy for a 0.7 mfp Pu-239 sphere (DM118).

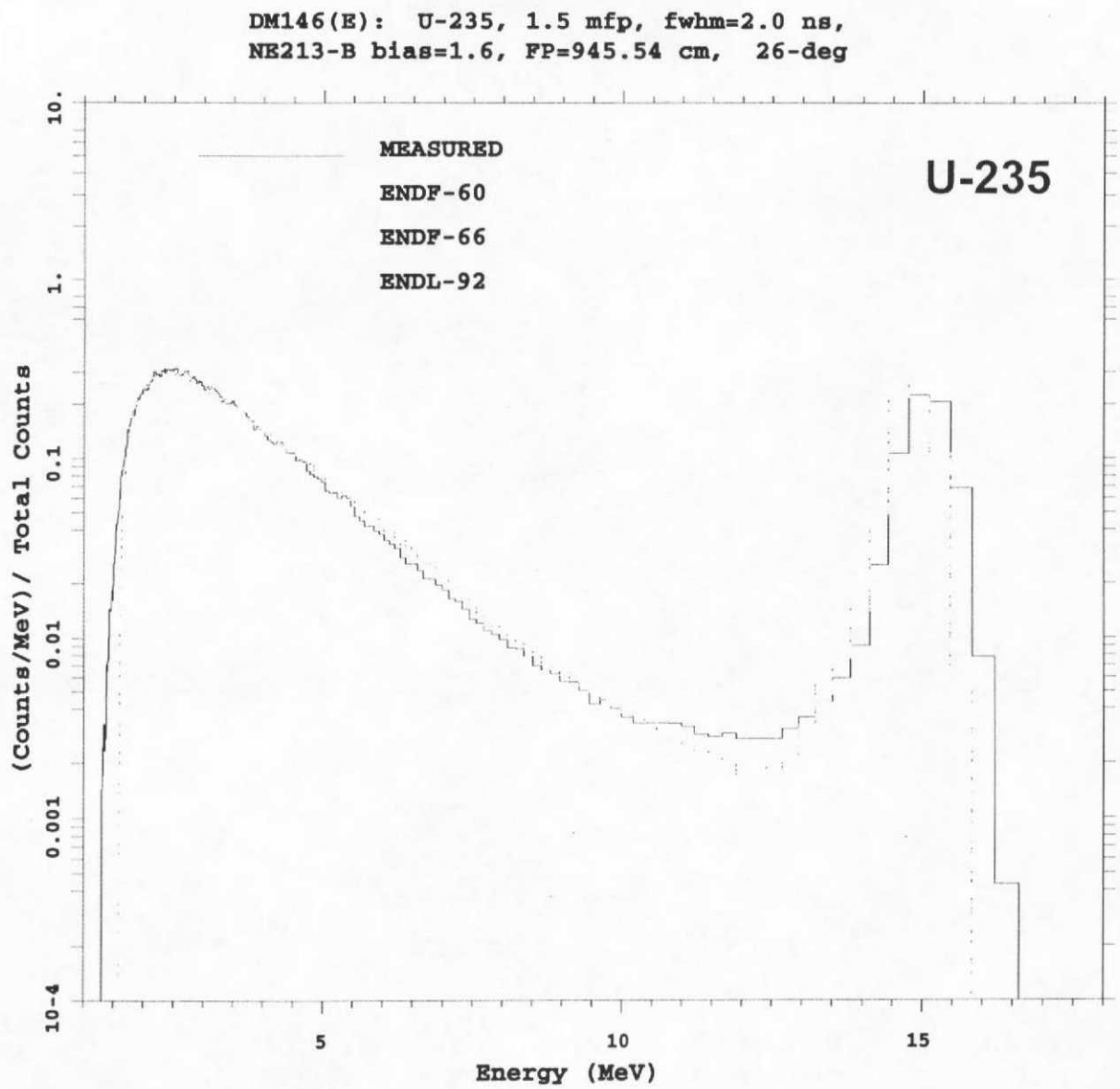

Fig. 59b. Comparison of results vs energy for a 1.5 mfp U-235 sphere (DM146).

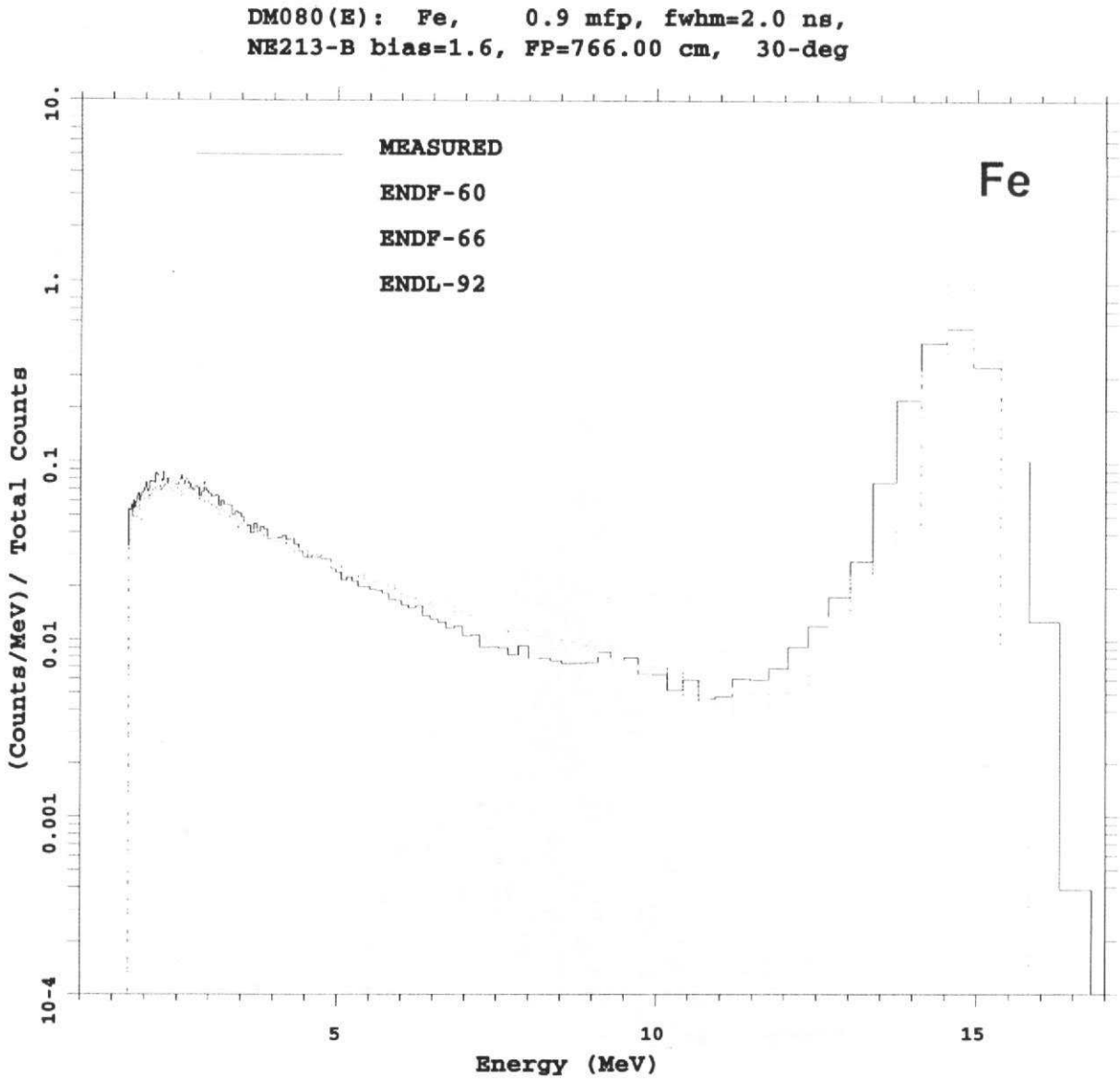

Fig. 50b. Comparison of results vs energy for a 0.9 mfp Iron sphere (DM080).

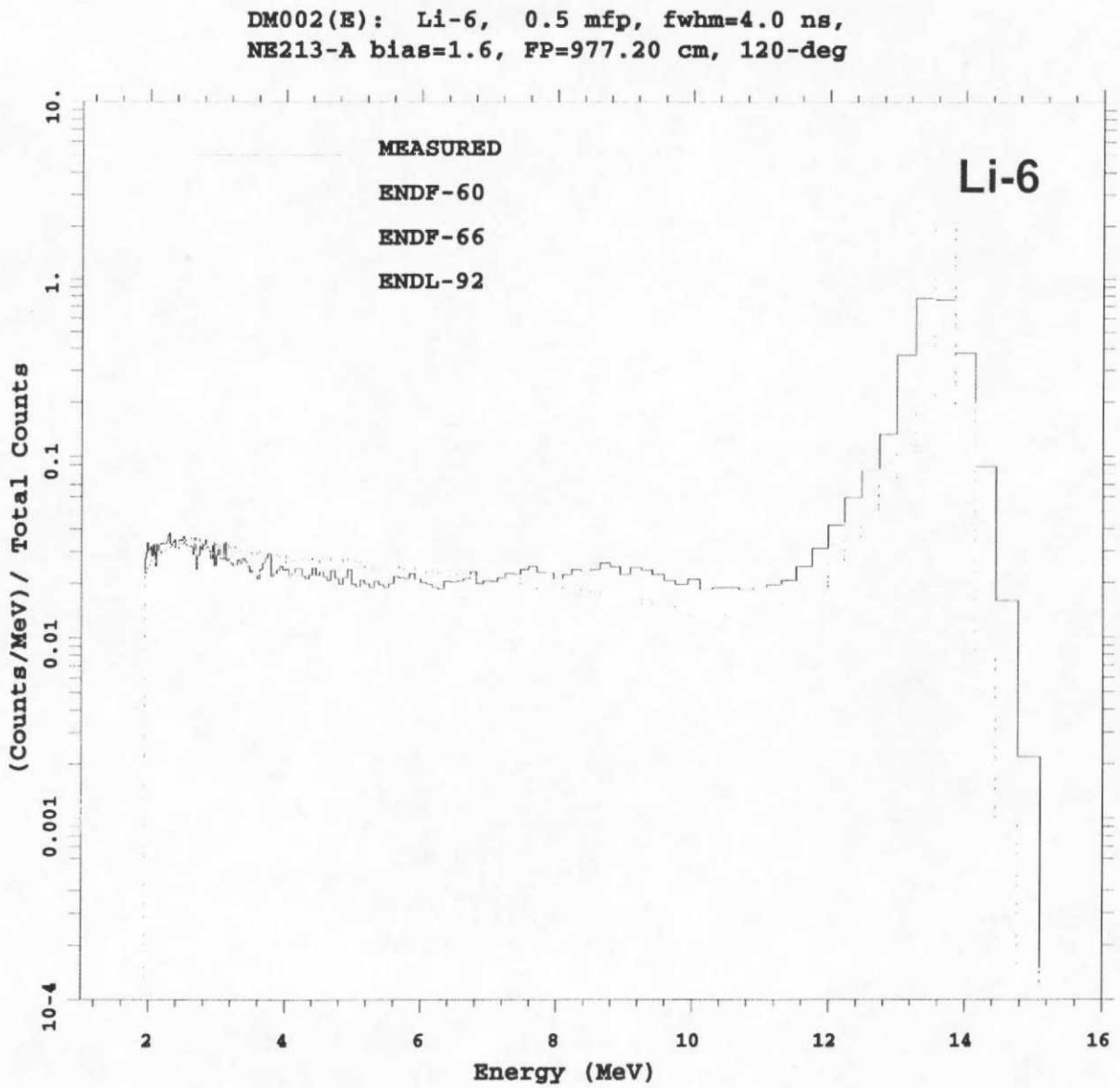

Fig. 43b. Comparison of results vs energy for a 0.5 mfp Li-6 sphere (DM002).

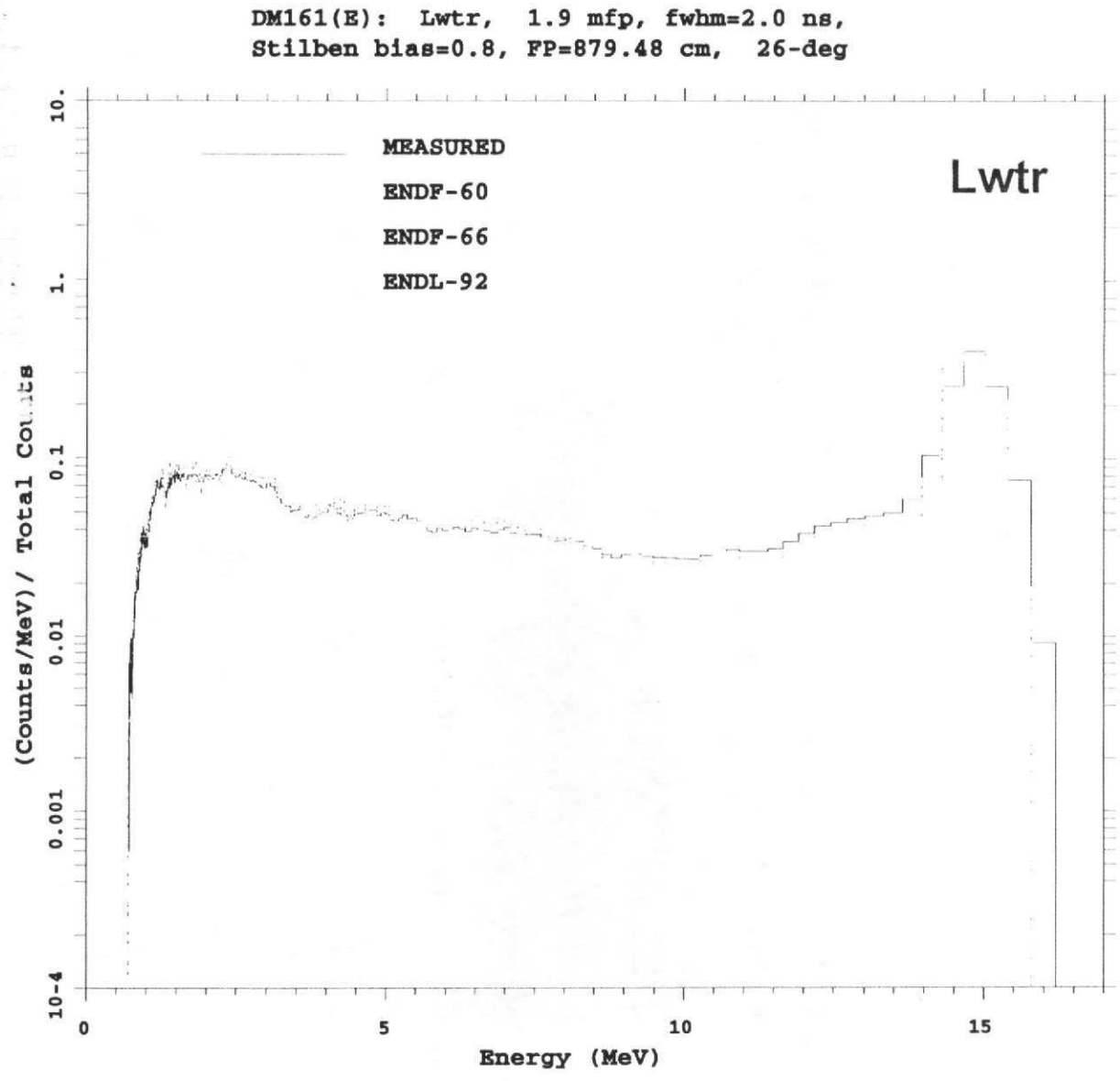

Fig. 62b. Comparison of results vs energy for a 1.9 mfp Light Water sphere (DM161).

Final Results – comments on comparisons

- **Generalizations are subjective and hard to make when you have 76 det measurements on 36 sphere configurations made of 20 different materials, and measurements were made with 8 different kinds of detectors in 3 different beamtubes.**

- **Results for each case should be judged separately. Nevertheless, the table on next slide helps a lot.**

Generally speaking:

- **The ENDL92 data seems to do better than ENDF at higher energies (E > about 10 MeV) where flight times are less than 200 ns.**

- **The ENDF data seems to do better than ENDL92 at lower energies (E < about 10 MeV) where flight times are more than 200 ns.**

- **The ENDF60 and ENDF66 results generally appear to be indistinguishable for the materials, energies, and flight times studied.**

Table used to judge final comparison plots

Table 11. Summary of comparisons between the calculated pulsed-sphere results using the ENDF60, ENDF66, and ENDL92 cross sections based on the final comparison plots for the 76 detector measurement calculations performed to date. Comparisons are made separately for the very high energy range (E > about 10 MeV) with flight times less than 200 ns, and the for lower energies (E < about 10 MeV) with flight times greater than 200 ns. The following six symbols are used in the second and third columns to indicate the findings in each energy range:

L=ENDL is better than ENDF, F=ENDF is better then ENDL, *=ENDL & ENDF about equal;
0=ENDF60 better than ENDF66, 6=ENDF66 better than ENDF60, i=60/66 indistinguishable.

Det Meas. ID #	Short Times <200ns	Long Times >200ns	MCNP Input File	Sph Matl	Size (mfp)	Outer Radius (cm)	FWHM (ns)	Beam Line ID	Beam Ang wrt the Src(deg)	Flight Path (cm)	Detector Type	Det Bias MeV
DM001	Li	Li	6Li0.5a	Li-6	0.5	8.970	4	30	38.8877	765.2	Pilot B	1.6
DM002	Li	*i	6Li0.5b	Li-6	0.5	8.970	4	120	116.7050	977.2	NE213-A	1.6
DM003	Li	Li	6Li0.5c	Li-6	0.5	8.970	2	26	26.0	746.34	NE213-B	1.6
DM007	*i	Li	6Li1.6a	Li-6	1.6	25.520	4	30	38.8877	765.2	Pilot B	1.6
DM008	Li	Li	6Li1.6b	Li-6	1.6	25.520	2	26	26.0	746.34	NE213-B	1.6
DM009	*i	Fi	7Li0.5a	Li-7	0.5	8.970	4	30	38.8877	765.2	Pilot B	1.6
DM010	Li	Li	7Li0.5b	Li-7	0.5	8.970	4	120	116.7050	977.2	NE213-A	1.6
DM011	Li	*i	7Li0.5c	Li-7	0.5	8.970	2	26	26.0	746.34	NE213-B	1.6
DM015	*i	Fi	7Li1.6a	Li-7	1.6	25.520	4	30	38.8877	765.2	Pilot B	1.6
DM016	Li	Fi	7Li1.6b	Li-7	1.6	25.520	2	26	26.0	746.34	NE213-B	1.6
DM033	F6	F0	AL0.9a	AL	0.9	8.940	4	30	38.8877	765.2	Pilot B	1.6
DM034	F6	L0	AL0.9b	AL	0.9	8.940	4	120	116.7050	977.2	NE213-A	1.6
DM036	F0	F0	AL2.6	AL	2.6	25.500	4	30	38.8877	765.2	Pilot B	1.6
DM039	*i	*i	Be0.8a	Be-9	0.8	12.580	4	30	38.8877	765.2	Pilot B	1.6
DM040	*i	*i	Be0.8b	Be-9	0.8	12.580	2	26	26.0	878.0	Stilbene	0.8
DM041	*i	*i	Be0.8c	Be-9	0.8	12.580	2	26	26.0	728.0	NE213-C	0.8
DM042	*i	*i	Be0.8d	Be-9	0.8	12.580	2	26	26.0	728.0	Stilbene	0.8
DM043	*i	*i	Be0.8e	Be-9	0.8	12.580	2	26	26.0	728.0	NE213-C	3.0
DM044	*i	*i	Be0.8f	Be-9	0.8	12.580	2	26	26.0	728.0	Stilbene	3.0
DM060	Fi	Fi	C0.5a	C	0.5	4.187	4	30	38.8877	766.0	NE213-A	1.6
DM061	*i	Fi	C0.5b	C	0.5	4.187	4	120	116.7050	975.2	NE213-A	1.6
DM064	Fi	Fi	C2.9a	C	2.9	20.960	4	30	38.8877	766.0	NE213-A	1.6
DM065	Fi	Fi	C2.9b	C	2.9	20.960	4	120	116.7050	975.2	NE213-A	1.6
DM066	*i	*i	POL0.8a	Poly	0.8	16.500	2	26	26.0	878.0	Stilbene	0.8
DM114	*i	*i	POL0.8d	Poly	0.8	16.500	6	30	38.8877	754.0	Pilot B	1.6
DM116	*i	*i	POL3.5	Poly	3.5	40.400	4	30	38.8877	765.0	Pilot B	1.6
DM071	*i	*i	Con2.0a	Conc	2.0	21.000	3	120	116.7050	975.4	NE213-A	1.6
DM072	*i	Fi	Con2.0b	Conc	2.0	21.000	2	120	116.7050	975.4	NE213-B	1.6
DM073	*i	*i	Con3.8a	Conc	3.8	35.500	3	120	116.7050	975.4	NE213-A	1.6
DM074	*i	Fi	Con3.8b	Conc	3.8	35.500	2	120	116.7050	975.4	NE213-B	1.6
DM079	Fi	*i	Fe0.9a	Fe	0.9	4.460	3	30	38.8877	766.0	NE213-A	1.6
DM080	Li	Fi	Fe0.9b	Fe	0.9	4.460	2	30	38.8877	766.0	NE213-B	1.6
DM081	Fi	Fi	Fe0.9c	Fe	0.9	4.460	3	120	116.7050	975.2	NE213-A	1.6
DM085	Li	*i	Fe4.8a	Fe	4.8	22.300	3	30	38.8877	766.0	NE213-A	1.6
DM086	Fi	Li	Fe4.8b	Fe	4.8	22.300	3	120	116.7050	975.2	NE213-A	1.6
DM087	Fi	Li	Fe4.8c	Fe	4.8	22.300	2	30	38.8877	766.0	NE213-B	1.6
DM096	Fi	Li	Mg0.7a	Mg	0.7	8.940	4	30	38.8877	765.2	Pilot B	1.6
DM097	Li	Li	Mg0.7b	Mg	0.7	8.940	4	120	116.7050	977.2	NE213-A	1.6
DM099	Fi	Li	Mg1.9	Mg	1.9	25.500	4	30	38.8877	765.2	Pilot B	1.6
DM101	*i	Fi	N1.1a	L-Nit	1.1	19.050	5	30	38.8877	763.3	Pilot B	1.6
DM102	Li	Fi	N1.1b	L-Nit	1.1	19.050	3.7	26	26.0	782.3	Ne213-B	1.6
DM103	*i	Fi	N3.1	L-Nit	3.1	55.880	4	30	38.8877	765.2	Pilot B	1.6

Table 11 (cont)

Det Meas. ID #	Short Times <200ns	Long Times >200ns	MCNP Input File	Sph Matl	Size (mfp)	Outer Radius (cm)	FWHM (ns)	Beam Line ID	Beam Ang wrt the Src(deg)	Flight Path (cm)	Detector Type	Det Bias MeV
DM107	*i	*i	O0.7a	L-Oxy	0.7	10.480	5	30	38.8877	754.0	Pilot B	1.6
DM108	*i	*i	O0.7b	L-Oxy	0.7	10.480	3.5	26	26.0	782.3	NE213-B	1.6
DM110	Li	F0	Pb1.4a	Pb	1.4	8.970	3	30	38.8877	766.0	NE213-A	1.6
DM111	F6	F6	Pb1.4b	Pb	1.4	8.970	3	120	116.7050	975.2	NE213-A	1.6
DM117	Li	Fi	49P0.7a	Pu239	0.7	3.665	3	30	38.8877	766.0	NE213-A	1.6
DM118	Li	Fi	49P0.7b	Pu239	0.7	3.665	3	120	116.7050	975.2	NE213-A	1.6
DM119	Li	Fi	49P0.7c	Pu239	0.7	3.665	2	26	26.0	945.54	NE213-B	1.6
DM126	Li	*i	Tef0.9	Tef	0.9	16.500	6	30	38.8877	752.0	Pilot B	1.6
DM129	Li	Li	Tef2.9a	Tef	2.9	25.500	6	30	38.8877	752.0	Pilot B	1.6
DM130	Li	Li	Tef2.9b	Tef	2.9	25.500	3	120	116.7050	975.4	NE213-A	1.6
DM133	Fi	Li	Ti1.2	Ti	1.2	8.940	4	30	38.8877	765.2	Pilot B	1.6
DM135	Li	Li	Ti3.5	Ti	3.5	25.500	4	30	38.8877	765.2	Pilot B	1.6
DM136	*i	*i	W1.0a	W	1.0	10.360	4.1	26	26.0	801.4	NE213-B	1.6
DM139	*i	*i	W3.0	W	3.0	10.360	4.1	26	26.0	801.4	NE213-B	1.6
DM140	Li	Fi	25U0.7a	U-235	0.7	3.195	3	30	38.8877	766.0	NE213-A	1.6
DM141	Li	Fi	25U0.7b	U-235	0.7	3.195	3	120	116.7050	975.2	NE213-A	1.6
DM142	Li	Fi	25U0.7c	U-235	0.7	3.195	2	26	26.0	945.54	NE213-B	1.6
DM143	Li	Fi	25U1.5a	U-235	1.5	5.938	3	30	38.8877	766.0	NE213-A	1.6
DM144	Li	Fi	25U1.5b	U-235	1.5	5.938	3	120	116.7050	975.2	NE213-A	1.6
DM145	Li	Fi	25U1.5c	U-235	1.5	5.938	2	26	26.0	879.0	Stilbene	0.8
DM146	Li	Fi	25U1.5d	U-235	1.5	5.938	2	26	26.0	945.54	NE213-B	1.6
DM149	Li	*i	28U0.8a	U-238	0.8	3.630	4	30	38.8877	765.2	Pilot B	1.6
DM150	Fi	*i	28U0.8b	U-238	0.8	3.630	4	120	116.7050	977.2	NE213-A	1.6
DM151	F0	*i	28U0.8c	U-238	0.8	3.630	2	26	26.0	945.54	NE213-B	1.6
DM153	F0	Li	28U2.8a	U-238	2.8	10.932	4	30	38.8877	765.2	Pilot B	1.6
DM154	Fi	Fi	28U2.8b	U-238	2.8	10.932	2	26	26.0	746.34	NE213-B	1.6
DM157	*i	*i	Hwt1.2	HWtr	1.2	10.480	5	30	38.8877	765.2	Pilot B	1.6
DM078	Fi	Fi	Hwt2.1	HWtr	2.1	19.050	5	30	38.8877	765.2	Pilot B	1.6
DM155	*i	*i	Lwt1.1a	LWtr	1.1	10.480	5	30	38.8877	754.0	Pilot B	1.6
DM156	*i	*i	Lwt1.1b	LWtr	1.1	10.480	2	26	26.0	731.52	NE213-B	1.6
DM158	*i	*i	Lwt1.9a	LWtr	1.9	19.050	5	30	38.8877	754.0	Pilot B	1.6
DM159	*i	*i	Lwt1.9b	LWtr	1.9	19.050	3	120	116.7050	975.4	NE213-A	1.6
DM160	*i	*i	Lwt1.9c	LWtr	1.9	19.050	2	26	26.0	731.52	NE213-B	1.6
DM161	*i	*i	Lwt1.9d	LWtr	1.9	19.050	2	26	26.0	879.48	Stilbene	0.8

Conclusion

Technical Conclusions

- Including collimator changes character of calculated results relative to the early sea-of-air models, esp in 10-12-MeV range for heavy spheres; calculated results are now more depressed in this energy valley.
- Including full concrete wall of vault has virtually no noticeable effect if collimators are already in the model.
- Marchetti's new source yields much better results in 12-15 MeV range than the traditional (old) source specifications; new is recommended.
- Results for concrete vs black collimators were inconclusive for the RZ-symmetric models with ring detectors; used black here.
- ENDL slightly better than ENDF above 10 MeV; ENDF better below 10; difficult to generalize; better to look at plots for individual cases.
- Generally no noticeable differences between ENDF60 & ENDF66 results.
- In the future, true 3-D models with "cylindrical" beamtubes and DXTRAN spheres to better sample collisions in the concrete collimators may (?) improve results in the 10.5 to 12.5 MeV region and/or resolve questions.

Final Remarks & New Reports

- A comprehensive Master Library has been developed with information and experimental data for 145 detector measurements made on 75 pulsed-sphere configurations made of 32 different materials.

  -- See "A Master Library of High-Energy Measurements from the LLNL Pulsed Sphere Program," ORNL/TM-2003/92 (March 2003)

- Extensive parametric calculations have been performed to evaluate proposed enhancements before upgrading the MCNP models.

- Comparison calculations based on the final models and the ENDF60, ENDF66, and ENDL92 xsect data have been performed for 76 detector measurements on 36 different spheres made of 20 different materials.

  -- See "Updated MCNP Analyses of High-Energy Measurements from the LLNL Pulsed Sphere Program," ORNL/TM-2003/121 (April 2003)

- Both reports, with "all" comparison plots, are /will be/ available on CD-ROM.